2050 Outlook for Forestry Residue-Based SAF in the Netherlands

Comparative Analysis of Gasification Fischer-Tropsch and Hydrothermal Liquefaction

Mark Willem ter Heide

Delft University of Technology

TU Delft

2050 Outlook for Forestry Residue-Based SAF in the Netherlands

Comparative Analysis of Gasification Fischer-Tropsch and Hydrothermal Liquefaction

by

Mark Willem ter Heide

Project Duration: February, 2025 - September, 2025
Faculty: Faculty of Aerospace Engineering, Delft

TU Delft

Contents

1

Scientific Article

2050 Outlook for Forestry Residue-Based SAF in the Netherlands: Comparative Analysis of Gasification Fischer-Tropsch and Hydrothermal Liquefaction

MW ter Heide, *AE Master Student*

Delft University of Technology, Delft, Netherlands

Decarbonizing the aviation industry has become a major focus of attention, which still is 99.7% reliant on fossil-based fuel. A promising solution is the production of Sustainable Aviation Fuel (SAF) from secondary biomass feedstocks such as forestry residues. For the Netherlands, studies estimate a substantial supply of forestry residues for bioenergy purposes by 2050. This study addresses the question under which conditions SAF production from forestry residues can become economically feasible in the Dutch context. Thermochemical pathways including Gasification Fischer-Tropsch (GFT) and Hydrothermal Liquefaction (HTL), followed by dedicated SAF refinery processes, offer potential conversion routes. However, a comparative techno-economic analysis for this context is lacking, and existing studies often neglect the effects of technological learning and CO_2 capture and storage on performance outcomes. This study evaluates feasibility by comparing the techno-economic performance of GFT and HTL. Process designs for both pathways are developed and these are side-by-side assessed on technical performance, cost structure, sensitivity to key parameters, and two potential scenarios. Results show that HTL achieves 47% higher SAF yields (18.3%) and a lower minimum fuel selling price (MFSP) of €1.03/L compared to GFT (10.2% yield and €1.49/L MFSP). Nonetheless, under the base scenario both pathways remain uncompetitive with fossil kerosene (€0.50/L). However, under the optimum progressive scenario, HTL achieves competitiveness with an MFSP of €0.30/L, while GFT reaches €0.50/L, positioning HTL as the more promising pathway in the Dutch context. However, supportive policy frameworks are needed to accelerate deployment of these technologies.

1 Introduction

Pre-COVID, direct greenhouse gas (GHG) emissions from the transport sector accounted for 23% of total global emissions, with aviation responsible for 12% of transport-related emissions [1]. Following a brief decline, CO_2 emissions are projected to surpass their 2019 levels by 2025 [2]. This trend is driven largely by the sector's near-total reliance (99.7%) on fossil-based kerosene and the growing demand for air travel [3]. Reducing air travel demand is often viewed as a difficult and short-sighted measure, making the transition away from fossil fuels a more viable decarbonization strategy for the short- and long term.

Promising non-emitting propulsion technologies, such as electric aircraft for short-haul flights and hydrogen propulsion for medium-haul flights, offer potential solutions [4, 5]. However, these technologies remain far from large-scale deployment. In the short term, the most viable approach is to transition the fuel source from fossil-based kerosene to renewable alternatives, collectively known as Sustainable Aviation Fuel (SAF) [6]. Growing interest in SAF is driven by international policy targets mandating its progressive blending with fossil kerosene. In particular, the European Union's ReFuelEU Aviation mandate requires that SAF usage at EU airports increase from 2% in 2025 to 70% by 2050 [7].

A readily available short-term option for SAF production is the use of waste and residue lipids, such as used cooking oil (UCO) or animal fats. These feedstocks can be converted into fuels via the hydroprocessed esters and fatty acids (HEFA) pathway, which involves relatively simple cleaning and filtering steps. Multiple HEFA production facilities are already operational [8, 9]. However, feedstock availability is limited, making HEFA suitable only for meeting short-term SAF demand. **Blanshard et al.** [10]

estimate that HEFA could supply at most 8% of global SAF demand by 2050.

Beyond HEFA, early-generation biofuels derived from food crops have also been proposed. However, these fuels are associated with several drawbacks, including net energy losses, increased GHG emissions, and rising food prices [11]. These concerns have shifted attention toward the development of advanced biofuels produced from non-food feedstocks. Among these, lignocellulosic feedstocks, particularly forestry residues, are well studied and offer several advantages, including high feedstock availability, relatively low cost, low ash content, and the ability to produce high-quality oil [12].

These feedstocks can be converted into biofuels through several thermochemical conversion technologies currently under development, including Gasification Fischer-Tropsch (GFT), Hydrothermal Liquefaction (HTL), and Fast Pyrolysis (FP). In GFT, the feedstock is first dried and reduced in size to optimize process efficiency and fuel yield. The pretreated feedstock is then converted into syngas, a mixture of CO and H_2, through partial oxidation at high temperatures (600–1000°C). This syngas undergoes catalytic FT synthesis to produce syncrude, which can be subsequently refined into fuels. In HTL, the feedstock is mixed and preheated with water to form a slurry, which is maintained at elevated temperature and pressure (300–400°C, 50–200 bar) to break down complex biomass structures into a bio-oil product that requires upgrading. HTL is particularly effective for feedstocks with high moisture content, as water serves as the reaction medium [13]. This makes HTL well suited for forestry residues, which typically contain around 50% moisture [14, 15, 16]. In FP, the feedstock is also dried and reduced in size as pretreatment. The biomass is then rapidly heated in the absence of oxygen (450–600°C), producing bio-oil, non-condensable gases, and char, with bio-oil serving as the primary product for subsequent upgrading [17].

Comparative studies indicate that GFT outperforms FP in terms of mass (14% vs 9%) and energy yields (43% vs 26%) as well as SAF production price for biomass-to-SAF conversion (€2.58/L vs €3.78/L) [18, 19]. Similarly, HTL has been shown to outperform FP in mass (14% vs 12%) and energy balances (62% vs 54%) and biofuel production price for biomass-to-biofuel conversion (€0.62/L vs €0.96/L) [15, 20]. Based on these early findings, this study focuses on the comparison of GFT and HTL for SAF production.

The oil products generated by these processes, syncrude from GFT and bio-oil from HTL, do not yet meet the specifications of drop-in SAF. Therefore, additional upgrading steps in a subsequent refinery process are required to meet SAF standards. This is followed by product separation into fractions for jet fuel, and gasoline.

Several studies have assessed the techno-economic performance of biomass conversion for individual pathways. **Tzanetis et al.** [20] analyzed biomass-to-biofuel conversion via HTL by considering changes in three reaction variables such as catalyst use, temperature, and catalyst/biomass mass ratio. Processing capacity was set to 1000 t_{db}/d and internal hydrogen production was incorporated for internal refinement utilization. Although the product mix included SAF, no refinery design for maximizing SAF output was considered. Production costs were reported, but the analysis lacked key financial metrics such as the internal rate of return (IRR) and did not calculate the minimum fuel selling price (MFSP). **Snowden-Swan et al.** [21] studied a HTL plant (100 t_{db}/d) located next to a waste water treatment plant for converting waste water slurries into hydrocarbon blendstock. Internal hydrogen- and electricity production is incorporated in the design. It provides a more comprehensive economic analysis, reporting an MFSP of €0.80/L, but focused exclusively on diesel and naphtha rather than SAF. **Kumar et al.** [22] targeted SAF production from waste-water grown algae via HTL. No internal electricity- or hydrogen production was included. The study resulted in a MFSP of €2.04/L; however, this study considered a first-of-a-kind (FOAK) plant with a processing capacity of 100 t_{db}/d. In contrast, **Deuber et al.** [23] assessed a commercial-scale HTL SAF plant (1,124 t_{db}/d) located in Brazil using sugarcane residues with internal hydrogen production, and reported an MFSP between €1.02/L and €1.20/L.

For GFT, more studies have been conducted specifically on SAF production at commercial scale. **Michailos et al.** [24] designed a commercial scale plant (2400 t_{db}/d) with a combined heat and power (CHP) system and **Tanzil et al.** [25] designed a commercial scale plant (1032 t_{db}/d) with electricity production. They reported MFSP values of €1.97/L and €1.65–2.37/L, respectively.

Fewer studies directly compare GFT and HTL. **Zhu et al.** [14] and **Tanzer et al.** provide comparative analyses, but neither study specifically targeted SAF production. **Zhu et al.** considered a commercial-scale plant of 2000 t_{db}/d forestry residue feed with a steam cycle acting as a CHP system. It reported a diesel price of €0.97/L and €0.54/L for GFT and HTL respectively. **Tanzer et al.** analyzed a FOAK plant (500 t_{db}/d) where nine agroforestry residue feedstocks were considered. The process included a 'cogeration' system for GFT and HTL where electricity is produced from waste gases and solids. HTL also included a hydrogen production plant. The study did not include an IRR in their calculations, limiting the assessment of financial feasibility.

Overall, literature lacks a comparative study that evaluates both GFT and HTL with a focus on maximizing SAF production in a techno-economic context. Existing studies generally assume plants operating in the year of analysis, which may not reflect future market conditions, as most SAF facilities are expected to be commissioned after 2030 in response to regulatory-driven demand growth. Additionally, most studies assume that offgases containing CO_2 are vented to the atmosphere. With the implementation of the EU Emissions Trading System (EU ETS) [26], large emitters are being incentivized to mitigate CO_2 emissions, yet this is rarely incorporated into process designs.

Given the lack of studies for the Dutch situation, the scale of Schiphol Airport, and the frontrunner position of KLM Royal Dutch Airlines in SAF adoption, which uses

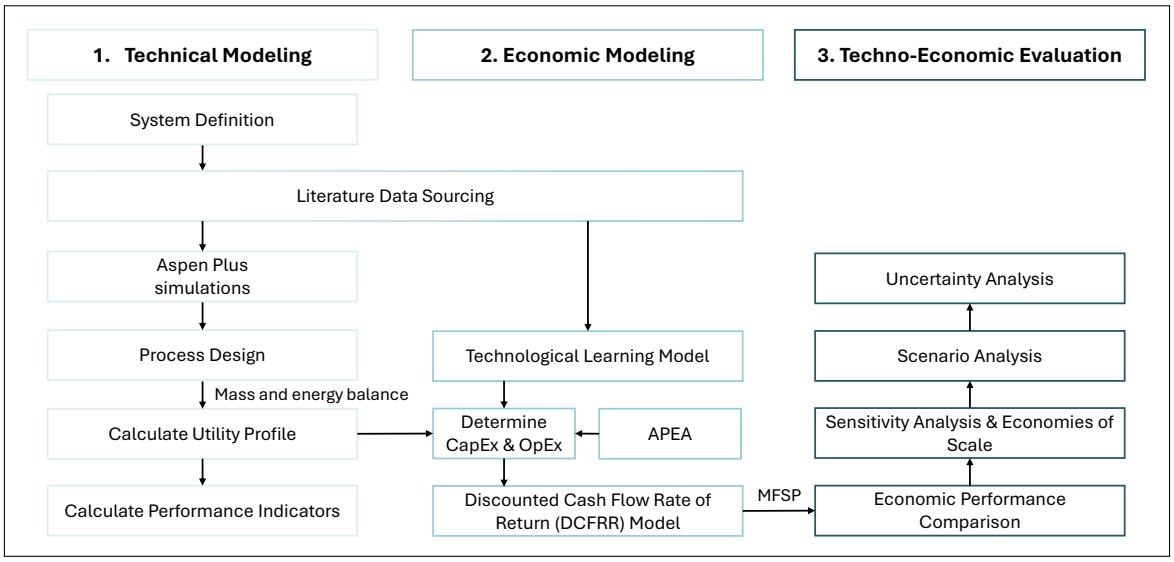

Fig. 1. The methodology comprises of three sequential phases: Technical Modeling, Economic Modeling, and Techno-Economic Evaluation.

Schiphol as its home base, it makes it an interesting location for SAF production [27].

Boosten et al. [28] projected the future availability of woody biomass in the Netherlands under multiple scenarios for 2050. The study estimated an annual supply of 1,324 kilotons (dry basis) of woody biomass for bio-energy applications.

Theoretically, this biomass could supply up to 4.4% of the Netherlands' total SAF demand in 2050, based on reported biomass-to-SAF yields available in literature [29, 18]. However, fuel yield alone is insufficient to assess the viability of these pathways.

The potential of these technologies to scale SAF production ultimately depends on their economic feasibility and competitiveness with fossil-based jet fuel (Jet A1) and HEFA-based fuel, which is priced at approximately €0.50/L and €1.67/L respectively [30].

This study evaluates and compares the techno-economic feasibility of gasification Fischer-Tropsch (GFT) and hydrothermal liquefaction (HTL) pathways for producing SAF from forestry residues in the Netherlands by 2050, with consideration of CO_2 mitigation and including technological learning rates.

System and process designs for both pathways were developed by aggregating and adapting designs, while ensuring streamlined process assumptions, from current literature. This was complemented with updated process variables and additional process units to make the design more representable for the current standard. The SAF refinery design was further refined using dedicated simulations and experimental data from literature. Finally, the techno-economic feasibility is assessed by a side-by-side assessment of technical- and economic performance, sensitivity to key parameters, and performance under different scenarios. And thereby offering insights into which pathway is more feasible in the Dutch context.

2 Methodology

The methodology used for the techno-economic analysis is outlined in Figure 1. The approach comprises three sequential phases: Technical Modeling, Economic Modeling, and Techno-Economic Evaluation.

Technical modeling is conducted to qualitatively define the system boundaries, and to quantitatively describe the process designs of two pathways: Gasification Fischer-Tropsch (GFT) and Hydrothermal Liquefaction (HTL).

The modeling begins with a system definition containing assumptions and system boundaries. Assumptions include decision on thermochemical pathway (GFT and HTL with SAF refinery), geographic location (Netherlands), temporal context (2050), economic base year (2024), process scale (N^{th}-of-a-kind plant: 2000 t_{db}/d), operating hours (8000 h/y), feedstock (forestry residues), and target product (SAF). These assumptions are established to contextualize the system. System boundaries determine which unit operations are included or excluded, meaning which operations are designed and which are only accounted for in the economic model.

Once the system was defined the process designs were developed by sourcing unit process data from literature. Data of different literature sources were evaluated for similar process assumptions to ensure that the aggregated data represents a coherent unit process design. Selection of data focused on finding similar data quality for both pathways, and standardization was prioritized above optimization of individual pathways. Gaps in the process design were filled with data from self simulated Aspen Plus models, for example the SAF refinery designs. Aspen Plus® Version 12 was used with Peng–Robinson equation of state as the property method for modeling the GFT SAF refinery, while the NRTL-RK model is applied for the HTL SAF refinery.

The process designs were quantitatively evaluated in a spreadsheet model developed in Microsoft Excel®. The following sections frequently reference this spead-

sheet model (Appendix A). An unit process approach was adopted, meaning a step-by-step description of process variables, mass- and energy balance, and utilities, per unit process block. It ensures a consistent level of detail across all blocks. The process simulates a single operational *train*, defined as one hour of continuous operation at a feedstock throughput of 2,000 t_{db}/d.

The process designs that are quantitatively described in the spreadsheet model yield the mass and energy balances. Then the utility profile, which represents consumption and production of utilities, such as electricity/steam/cooling water, is required for obtaining operational expenditures (OpEx) breakdown. Finally, performance indicators such as mass yields, carbon efficiency, thermal efficiency and E-factor can be calculated.

Economic modeling translates the technical model into a detailed breakdown of revenues and costs over a 20-year project lifetime. As novel technologies typically experience cost reductions through technological learning, these effects are incorporated on projections for an operational start date by 2050 [31]. Combined with the utility profile and data obtained from literature and Aspen Plus® Economic Analyzer (APEA), the model enables estimation of OpEx and capital expenditures (CapEx). The economic model structure is identical for both the GFT and HTL pathways. However, the underlying technical differences between the two thermochemical technologies lead to different parameter values within the model.

The economic performance is evaluated using a Discounted Cash Flow Rate of Return (DCFRR) method, where the minimum fuel selling price (MFSP) is calculated by setting the Net Present Value (NPV) to zero, including an Internal Rate of Return (IRR).

The techno-economic evaluation integrates and assesses the technical and economic results from the preceding phases by conducting a side-by-side comparison of the GFT and HTL pathways. Sensitivity analyses are performed to evaluate the impact of key technical and economic parameters as well as the effect of increasing process scale, leading to economies of scale. Subsequently, two future-oriented scenarios are analyzed to explore potential variations in MFSP, and required subsidy incentives. Finally, an uncertainty analysis was performed to assess the strengths, weaknesses and uncertainties of the data used as input for the technical and economic model.

The spreadsheet model was structured with a parallel data architecture to ensure that both thermochemical pathways were evaluated using a standardized set of assumptions and parameters. This design facilitates consistent comparison and enables rapid evaluation of alternative inputs. The integration of process and economic models ensures that modifications in the process model are automatically reflected in the economic outputs.

3 Technical Modeling

The system definition is represented by a set of assumptions and boundaries. The economic base year is set to 2024, as it is the most recent year with available inflation data. The monetary value used is the Euro (€). To the extent that data availability allowed, price levels and economic assumptions were aligned with economic conditions in the Netherlands. The system is designed for an n^{th}-of-a-kind (NOAK) plant operating from 2050, representing a commercial-scale facility with a processing capacity of 2,000 tons of dry biomass per day and an annual operating time of 8,000 hours.

Figure 2 defines the system boundaries for both thermochemical pathways, distinguishing between processes that fall within and outside the modeled system. While no process designs are developed for operations outside the system boundary, such as CO_2 storage and waste(water) treatment, their associated costs are included in the economic model as part of the OpEx. This section describes the processes included within the system boundaries of both the GFT and HTL pathways. It provides a step-by-step explanation according to the process flow design presented in Figure 3, with each stage referenced by its corresponding unit process block section labeled as *Block*.

The SAF refinery designs for both the GFT and HTL pathways take into account that jet fuel specifications are not highly restrictive with respect to molecular composition. The key composition-related criteria for refining jet fuel from FT synthesis include a freezing point below –47∘C, a carbon number range of C9–C15, and an aromatic content between 8–25 vol% [32].

3.1 Feedstock availability

As outlined in Figure 2, both thermochemical pathways consider biomass forestry residues as feedstock. GFT process design is mainly based on the design by **Zhu et al.** [14], which utilizes hybrid poplar wood as the feedstock. In contrast, the HTL rely on the work of **Tews et al.** [15], where chipped forest residues are employed. The ultimate analyses of both feedstocks are presented in Table 1, demonstrating comparable chemical compositions. This similarity confirms the suitability of the selected feedstocks for cross-technology comparison.

Table 1. Ultimate analysis of feedstocks for GFT (Hybrid Poplar Wood) and HTL (Chipped Forest Residue).

	Hybrid Poplar Wood[a]	**Chipped Forest Residue[b]**
Composition, db[c] (wt%)		
Carbon	50.60	50.90
Hydrogen	6.08	6.00
Oxygen	40.75	41.30
Nitrogen	0.61	0.30
Sulfur	0.02	0.03
Chloride	0.01	0.00
Ash	1.93	1.50
Other properties		
Moisture content (wt%)	50.00	50.00
HHV (MJ/kg, db[c])	18.81	20.40

[a] [14] [b] [15] [c]dry basis

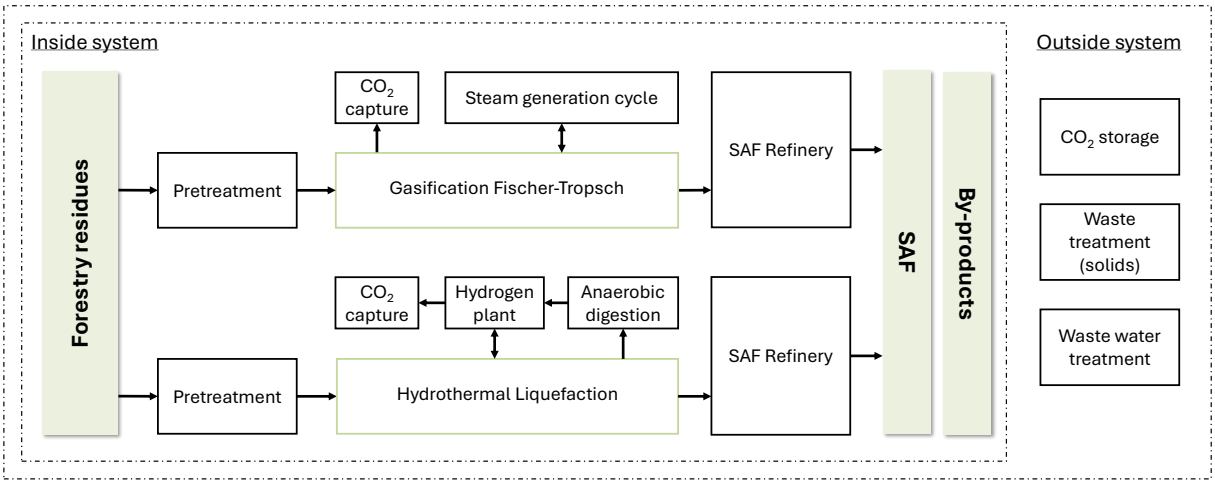

Fig. 2. System definition outlining the system boundaries.

3.2 Gasification Fischer-Tropsch

The resulting GFT process design is shown at the top of Figure 3. Corresponding to Figure 2, the following sections describe each process: *Blocks 1–3* cover the pretreatment process, *Blocks 4–10* the Gasification Fischer-Tropsch process, *Block 12* the steam generation process, *Block 13* the CO_2 capture process, and *Block 11* the SAF refinery.

Block 1-3: According to Table 1, the incoming feed, hybrid poplar wood, contains a moisture content of 50 wt%. Prior to gasification, this must undergo pretreatment operations. The moisture content must be reduced to 12 wt%. Drying is achieved using internal heat recovered from the gasification process. Following drying, the feedstock is subjected to grinding in order to increase its reactivity [11]. A particle size of 5 mm is assumed for the grinding step [33]. The dried and ground biomass is then fed into an indirectly heated gasifier.

Block 4-5: The indirectly heated gasifier consists of two coupled reactors: a gasifier, where feedstock is converted using hot sand and steam, and a combustor, where residual char is combusted to reheat the sand before re-entering the gasifier. In this study, the entire indirectly heated gasification system is modeled as a single unit process block. The gasification reactor operates at 870 ∘C and 1.6 bar [34, 35]. The primary gaseous output, syngas, is a mixture containing hydrogen (H_2) and carbon monoxide (CO), which are the target compounds for Fischer-Tropsch (FT) synthesis. It also includes carbon dioxide (CO_2), methane (CH_4), light hydrocarbons, tars, sulfur compounds, water vapor, and ammonia. Although tars are generally undesirable for downstream processes, they contain valuable carbon and hydrogen, which can be recovered. To facilitate this, tars are converted into H_2, CO, and light hydrocarbons in a tar reformer [34].

Block 6-7: The raw syngas is scrubbed with scrubber water to remove impurities like dissolved contaminants such as ammonia and residual tars. The waste water is treated outside the system in the waste water treatment (WWT) facility. Then the scrubbed gas is compressed where water is condensed and sent to the WWT. After compression, sulfur compounds are removed in a dedicated sulfur removal unit [34, 36].

Block 8-9: The cleaned syngas is processed in the steam reformer, where remaining tars, light hydrocarbons, and the majority of methane are converted into carbon monoxide (CO) and hydrogen (H_2) [37]. The water-gas shift (WGS) reactor then adjusts the H_2/CO ratio to the optimal value for the FT synthesis. In this study, an H_2:CO ratio of 2.1:1 is assumed. Following these steps, excess carbon dioxide (CO_2) and water are removed from the syngas stream, completing the final preparation step before it enters the FT reactor [34, 38].

Block 10: The FT process converts syngas into a hydrocarbon syncrude composed primarily of paraffins, olefins, and minor quantities of alcohols. **Zhu et al.** [14] present an oversimplified FT product profile that includes only paraffins in the syncrude composition. To obtain a more representative product distribution, the detailed composition provided by **A. de Klerk** [32] is adopted in this study. Both references assume a low-temperature FT (LTFT) reactor employing a cobalt-based catalyst, ensuring consistency in reactor configuration and operating conditions. To capture the chemical diversity of the syncrude, representative compounds are selected for each product subgroup (e.g., naphtha–olefins). An overview of the FT syncrude composition and the corresponding compound mapping is provided in Table 2.

Block 12: Steam generation cycle is modeled as a separate process in which excess process heat is recovered via heat exchangers. This recovered heat serves two primary functions: it is converted into electricity through a steam turbine generator, and it is used to produce superheated steam required by the gasifier and the steam reformer. An electrical conversion efficiency of 56% is assumed for the steam turbine [39]. To maintain continuous steam supply, the system incorporates a boiler that combusts fuel gas, as recovered process heat alone is insufficient to meet the total thermal demand. Additionally, the steam generation unit

Table 2. Detailed syncrude composition ([32]) and corresponding compound assumptions in the process design.

Detailed syncrude composition			Assumed compound
Gaseous product (C1–C4)	wt%	11.9	
methane	wt%	5.6	CH_4
ethane	wt%	1.1	C_2H_6
C3–C4 olefins	wt%	3.4	C_3H_6
C3–C4 paraffins	wt%	1.8	C_3H_8
Naphtha (C5–C10)	wt%	20.0	
olefins	wt%	8.0	C_8H_{16}
paraffins	wt%	12.0	C_8H_{18}
Distillate (C11–C22)	wt%	21.9	
olefins	wt%	1.1	$C_{15}H_{30}$
paraffins	wt%	20.8	$C_{16}H_{34}$
Residue/wax (C22+)	wt%	44.6	
paraffins	wt%	44.6	$C_{22}H_{46}$
Aqueous product	wt%	1.6	
alcohols	wt%	1.6	C_2H_6O

consumes water to produce the steam required for the gasification and steam reforming processes.

Block 13: To improve the environmental performance of the system, additional modules were implemented. Two CO_2 capture units, implemented as amine-based acid gas removal systems. Design parameters for these units were adopted from **Tan et al.** [38]. These CO_2 capture systems were integrated into the indirectly heated gasifier and the steam reformer & WGS unit process blocks.

3.2.1 GFT - SAF Refinery

Block 11: Based on the product distribution of **A. de Klerk** [32] the SAF refinery design was modeled. LTFT synthesis is preferable for SAF production, as a significant fraction of the syncrude naturally falls within the desired carbon number range.

First, the light fraction (C1-C5) was recovered and routed to the alkylation and oligomerisation process, where the carbon number is increased and benzene compounds are reduced. Two processes occur simultaneously: aromatic alkylation using benzene from *Block 11E* and olefin oligomerisation [40, 41]. Then, distillation extracts fuel gas which is used internally in *Block 8&12*. The resulting olefins are then hydrotreated to convert them into paraffins, as olefins are detrimental to fuel stability. The C6–C8 naphtha and lighter fractions from hydrocracking undergo aromatisation to further increase aromatic content before being split into fractions suitable for gasoline and jet fuel. Finally, the C9+ fraction is subjected to hydrocracking to shift the carbon distribution into the jet fuel range.

Furthermore, the refining process requires cooling water, steam, and hydrogen for both hydrotreating and hydrocracking reactions. The main byproducts include gasoline, liquefied petroleum gas (LPG). Unconverted organics and water, which are directed to wastewater treatment, and fuel gas, which is reused internally within the process.

3.3 Hydrothermal liquefaction

The resulting HTL process design is shown at the bottom of Figure 3. Corresponding to Figure 2, the following sections describe each process: *Blocks 1–2* cover the pretreatment process, *Blocks 3–6* the hydrothermal liquefaction process, *Block 9* the anaerobic digestion process, *Block 9* the hydrogen plant, *Block 10* CO_2 capture process, and *Block 7* the SAF refinery.

Block 1-2: The incoming feedstock, composed of forest residue biomass (Table 1), is first ground into fine particles. Although the biomass contains 50 wt% moisture, drying is not required, as HTL uses water as the reaction medium. Additional water is added to form the slurry and is later recovered and recycled within the process. The feed is preheated using heat recovered from heat exchangers, where hot reactor effluent heats the incoming feed. After preheating, the slurry is pressurized before entering the reactor.

Block 3: The preheated and pressurized slurry is then introduced into the HTL reactor, which operates at 203 bar and 355∘C [42]. A heater, fueled by process gases, supplies heat to a transfer fluid that maintains isothermal conditions within the reactor. Under these conditions, the biomass slurry is converted into an oil phase, an aqueous phase, gas mixture, and solid residues.

Block 4-6: Solids such as biochar and ash are removed from the reactor effluent through filtration. Ash is treated as waste, while biochar is assumed to be sold as a by-product. The liquid effluent from the filter is used to preheat the incoming biomass-water slurry via heat exchange, after which it is depressurized. Once cooled to 117∘C and depressurized to 1 bar, the stream enters a three-phase separator, producing a gas mixture, an aqueous phase, and an oil phase. The gas mixture consists of offgas (CO_2, CH_4, a litte H_2, C_2H_6, C_3H_8, C_4H_{10}), which is utilized for hydrogen production. The aqueous phase is further separated into two streams. One stream is recycled as process water for the HTL reaction, while the other, which contains dissolved organics, is sent to anaerobic digestion to generate additional offgas for hydrogen production. Any remaining water is directed to wastewater treatment. The oil phase is sent to the refinery for further upgrading.

Block 8: Dissolved organics present in the aqueous phase are converted in the anaerobic digestion reactor into CH_4 and CO_2. These gases are sent to the hydrogen plant, where they are used both as reformer feedstock and as fuel gas for fired heaters.

Block 9: The gas mixture is preheated using heat recovered from the reformer furnace. Simultaneously, recycle water from the biomass conversion and upgrading processes is heated by the flue gases from the furnace to generate saturated steam. This steam is then mixed with the preheated gas mixture, which is subsequently sent to the reformer operating at 31 bar and 850∘C. The reformed gas is cooled and directed to a separate shift reactor, where a WGS reaction is performed to further increase hydrogen

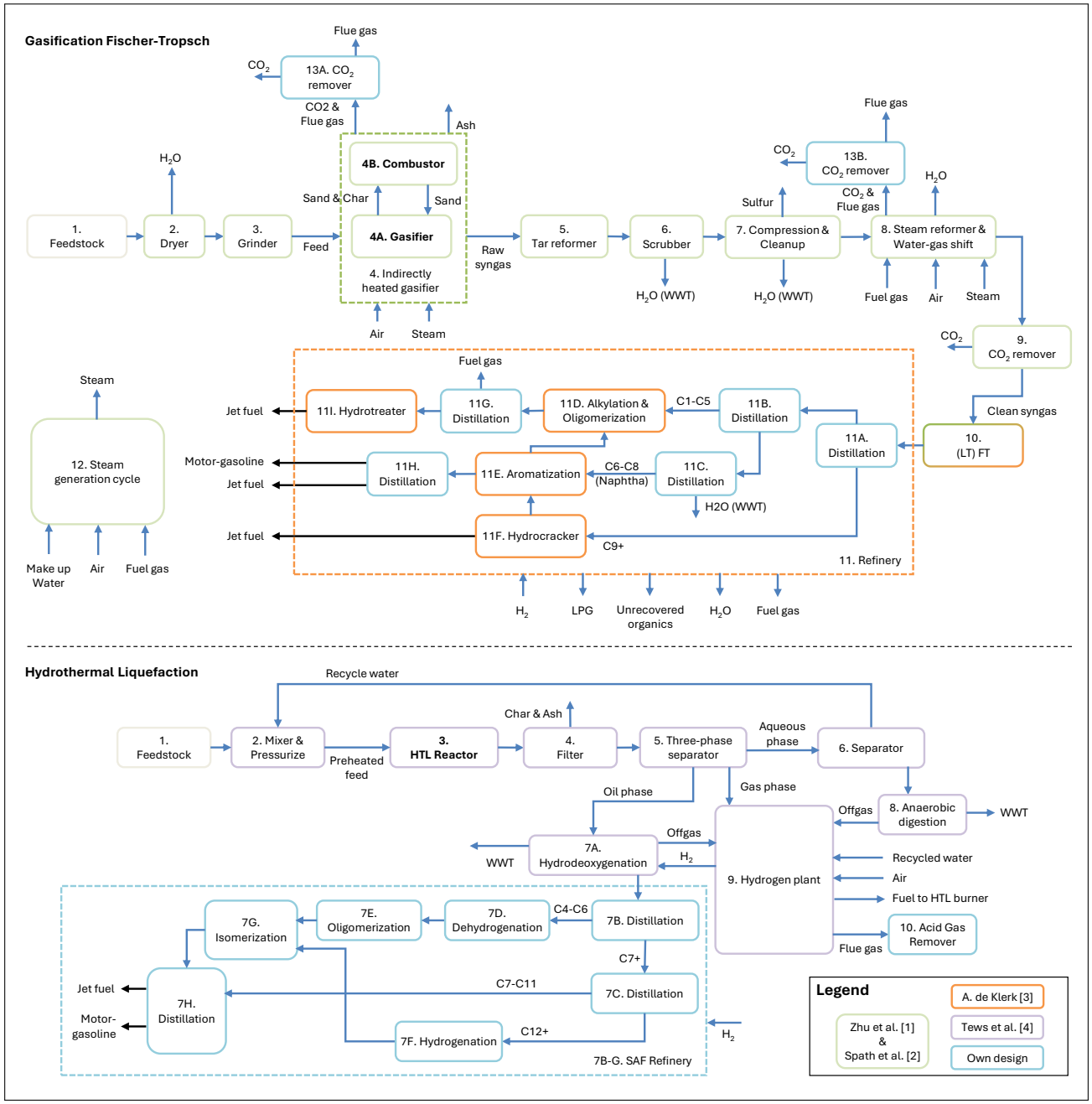

Fig. 3. The resulting process designs, where GFT is shown at the top, and HTL at the bottom. A unit process approach was used, ensuring a consistent level of detail across all process blocks. The legend indicates which design from literature is used for specific process sections.

production. After the shift reaction, the gas stream passes through a knock-out drum for water removal. Finally, hydrogen is separated from the gas mixture in a pressure swing adsorption (PSA) unit before being sent to the bio-oil upgrading reactor.

Block 10: Additional CO_2 removal units have been incorporated into the process design, and the captured CO_2 is assumed to be stored. For the CO_2 removal units, the design parameters of **Tan et al.** [38] are adapted.

3.3.1 HTL - SAF Refinery

Block 7: The first stage of the refinery process is hydrodeoxygenation, in which the oil phase is reacted with hydrogen over a NiMo catalyst until the oxygen content is reduced to below 1% [42]. Hydrogen supplied by the on-site hydrogen production unit is used for this purpose. In this study, additional processing modules are introduced to further upgrade the hydrodeoxygenated oil phase toward SAF.

The process begins with distillation of the hydrodeoxygenated oil to separate the C4–C6 paraffin fraction. As these lighter compounds fall below the carbon number range for jet fuel, their chain length is increased through oligomerisation. Prior to oligomerisation, the alkanes are dehydrogenated to alkenes via oxidative dehydrogenation at approximately 350∘C, where cyclohexane is converted

to cyclohexene and hydrogen [43]. Excess hydrogen is removed and subsequently used for hydrogenating the C12+ aromatic fraction. The alkenes obtained from dehydrogenation are then oligomerized at 75–80∘C to achieve the carbon number range required for jet fuel [44].

The remaining C7+ stream undergoes a second distillation. The C12+ fraction contains a high proportion of aromatics and is therefore hydrogenated at 300–390∘C and 70–120 bar, converting aromatics to cycloparaffins in the presence of hydrogen [45]. Off-site hydrogen is purchased for this step. The hydrogenated C12+ stream is subsequently combined with the oligomerised C4–C6 alkenes. This combined stream is then processed in a hydroisomerization unit at 300–360∘C under high hydrogen pressure to introduce molecular branching [46], thereby lowering the freezing point of the final fuel. The C7–C11 fraction from the second distillation is blended directly with the isomerized stream. After blending and isomerization, the process yields two primary products: jet fuel and gasoline. The refinery process requires hydrogen, cooling water, electricity, steam, and thermal oil.

4 Results

The results are structured according to the three phases outlined in Figure 1. The technical modeling presents the final mass and energy balances, utility profile, and performance indicators. The economic modeling addresses technological learning, CapEx and OpEx, and the MFSP derived from the cash flow model. The techno-economic evaluation includes a side-by-side economic comparison of the two thermochemical pathways, followed by sensitivity and scenario analyses to assess the impact of parameter changes and future developments on economic feasibility. Finally, the uncertainty analysis evaluates the robustness of the results.

4.1 Technical Modeling Results & Comparison

4.1.1 Mass and Energy Balances

Mass and energy balances are based on the law of conservation of mass and energy. It states that for any system closed to all transfers of matter the mass and energy of the system must remain constant over time. The mass balance accounts for feedstock inputs, intermediate flows in the gas, solid, liquid, and aqueous phases, and final outputs such as SAF and byproducts including gasoline, LPG, biochar and CO_2. The energy balance expresses the mass flows in energy units, alongside the work performed (e.g., power consumption per unit process) and the associated heat losses. The resulting mass and energy balances, along with the process variables associated with the operational parameters of each unit process, are provided in the spreadsheet model (see Appendix A).

4.1.2 Utility profile

From the mass and energy balances, a utility consumption–production profile is derived. The resulting utility profile is presented in Table 3. It quantifies the net consumption or production of utilities per operational *train* of feedstock. This profile forms a fundamental input for calculating the variable operating costs. When possible, heat exchangers were used to produce part of the utilities needed. For example in the GFT pathway the heat is converted into hot steam which is used within the process and excess steam is converted into electricity. This explains the netto production (23.77 MW) of electricity for GFT, comparing to a netto consumption (23.58 MW) for HTL. Furthermore, natural gas and olivine are exclusively used in GFT for *Block 8&12* and gasifier respectively. Hydrogen consumption for HTL SAF refinery is 7 times higher unless the hydrogen production, which delivers only a share of the full consumption. On the other hand, steam consumption for GFT SAF refinery is 33 times higher than HTL, unless the internal steam production.

To convert utility use into monetary terms, a unit price must be defined. It is assumed that utility consumption and production scale linearly with processing capacity, meaning a doubling of capacity results in a proportional change in utility demand or output.

Table 3. Utility profiles for GFT and HTL based on a process capacity of 2000 t_{db}/d.

Utility	Unit	GFT	HTL
Water	t/h	6432.12	297.96
Electricity			
Consumption	MW	31.06	23.58
Production	MW	54.83	–
Netto	MW	23.77	-23.58
Natural gas	t/h	1.27	–
Olivine	t/h	2.26	–
Hydrogen	t/h	0.08	0.54
Steam	t/h	100.68	3.05
Catalyst			
HZSM-5 (*Block 5 & Block 9*)	t/h	0.0034	0.0042
NiMo (*Block 7A*)	t/h	–	0.0109
ZnO (*Block 7*)	t/5y	26.87	–
Steam reformer (*Block 8*)	t/5y	25.17	–
LT shift (*Block 8*)	t/5y	35.95	–
HT shift (*Block 8*)	t/5y	43.14	–
Cobalt (*Block 10*)	t/2y	5.66	–
WWT	t/h	97.93	96.72
Ash disposal	t/h	2.59	1.25

Steam and cooling water from GFT/HTL SAF refinery are included and assumed not to be recycled. For HTL, thermal oil is assumed to be recycled and initial costs are included in component installation factors.

4.1.3 Performance Indicators

Table 4 presents key performance indicators derived from the mass and energy balances of the GFT and HTL pathways. Yield is defined as the ratio between the mass flow of the respective product stream and the mass flow of dry biomass. Carbon efficiency is calculated as the ratio of the molar carbon contained in the main product (SAF) and

byproducts (Gasoline, LPG, Biochar, CO_2) to the total molar carbon inflow. A distinction is made between system designs with and without carbon capture. In designs that exclude carbon capture, the CO_2 is assumed to be vented, and thus is excluded from the byproduct carbon accounting [47].

Table 4. Process performance indicators for GFT and HTL.

	GFT		**HTL**	
	Mass flow $[t/h]$	Yield	Mass flow $[t/h]$	Yield
Feedstock	82.1	100%	82.1	100%
Products				
SAF	10.2	12.5%	15.0	18.3%
Gasoline	3.6	4.3%	8.3	10.1%
LPG	0.3	0.3%	–	–
Biochar	–	–	7.1	8.6%
CO_2	104.6	127.4%	27.8	33.9%
CO_2 capture	Yes	No	Yes	No
Carbon efficiency	96.8%	28.8%	78.8%	60.6%
Thermal efficiency	36.4%	–	63.4%	–
E-factor (cEF)	0.847	7.129	1.683	3.225

With an identical dry biomass input of 82.1 t/h, the HTL pathway demonstrates higher product yields across both liquid fuel streams, SAF and gasoline (Table 4). Specifically, SAF yield for HTL is 18.3%, compared to 12.5% for GFT, differs significantly.

Carbon efficiency follows contrasting trends depending on the inclusion of CO_2 emissions capturing. When CO_2 is considered a byproduct (i.e., with carbon capture), GFT demonstrates superior carbon efficiency (96.8%) relative to HTL (78.8%). However, in designs without carbon capture, HTL outperforms GFT, with a carbon efficiency of 60.6% versus 28.8%. This reversal is driven by the substantially higher CO_2 emissions associated with the GFT pathway, amounting to 104.6 t/h (127.4% yield), compared to 27.8 t/h (33.9% yield) for HTL. The elevated CO_2 output in GFT results primarily from the gasification and steam reforming & WGS processes. Yields exceeding 100% are attributed to the large volumes of reaction air introduced during gasification and the steam reforming & WGS reactions, which contribute additional mass to the product stream.

Thermal efficiency is calculated according to the method of **Sangaré et al.** [48], defined as the ratio of total energy output in products and byproducts to the total energy input. Depending on whether electricity is consumed or produced, it is included either as part of the total energy input or as a byproduct. Thermal efficiency is higher in the HTL process, reaching 63.4% versus 36.4% for GFT. The efficiency does not change by excluding CO_2 capture units.

As shown in Figure 4, the energy output per ton of dry biomass also supports thermal efficiency superiority of HTL. It yields higher specific energy outputs in both SAF (7.86 GJ/t) and gasoline (4.46 GJ/t), relative to GFT (5.38 GJ/t and 1.91 GJ/t, respectively). This directly related Table 4, where higher mass yields for HTL in these products were seen. Electricity production from the steam turbine contributes positively (23.77 MW, Table 3) to GFT's total energy output (1.04 GJ/t). HTL produces an additional biochar (1.89 GJ/t), which can be sold as byproduct. On an annual basis, total energy output from HTL reaches approximately 9.33 PJ, surpassing GFT's 5.57 PJ.

E-factors is an important metric to assess the greenness of the process, represented by the amount of waste produced per amount of product. The simple E-factor (sEF) assumes that 90% of wastewater is recycled, which results in an overly optimistic metric. To address this, the complete E-factor (cEF) is used, where wastewater is not recycled and thus represents the upper bound of the E-factor [49]. The E-factors reported in Table 4 correspond to this complete metric. Without CO_2 capture, HTL achieves a lower cEF (3.225) than GFT (7.129), indicating less waste generation. When CO_2 capture is included, GFT has a lower cEF (0.847) compared to HTL (1.683). This improvement for GFT is driven by the large quantity of captured CO_2 that is sold as a byproduct, whereas in HTL the cEF also decreases due to CO_2 capture but to a lesser extent. Industry cEF values for bulk chemical production typically range between 7 and 35. In comparison, both GFT and HTL pathways demonstrate lower values, indicating that they are greener in terms of waste generation than conventional industrial counterparts [49].

4.2 Economic Modeling Results & Comparison

4.2.1 Technological Learning

Technological progress and experience are modeled empirically by relating the total capital investment (TCI) to cumulative experience, typically expressed in terms of cumulative production or the number of installed plants [50, 51]. Given that the plants are assumed to be deployed in 2050, a preceding period of technological learning must be accounted for. The one-factor learning curve approach is applied to estimate the resulting cost reductions [31].

$$C_t = C_0 \left(\frac{P_t}{P_0} \right)^{-b} \tag{1}$$

In this equation, C_t represents the total capital investment (TCI) of the technology at time t, and C_0 denotes the initial TCI at $t = 0$. The cumulative production at time t and at $t = 0$ are indicated by P_t and P_0, respectively. Following the methodology of **Van der Spek et al.** [50], the values for P_t and P_0 are based on the expected number of global NOAK plants operating in 2050 and the estimated number of first-of-a-kind (FOAK) plants in operation in 2024 [10, 52].

The exponent b is related to the progress ratio (PR), as defined in Equation 2. Each doubling of cumulative plants results in a reduction of the total capital investment (TCI)

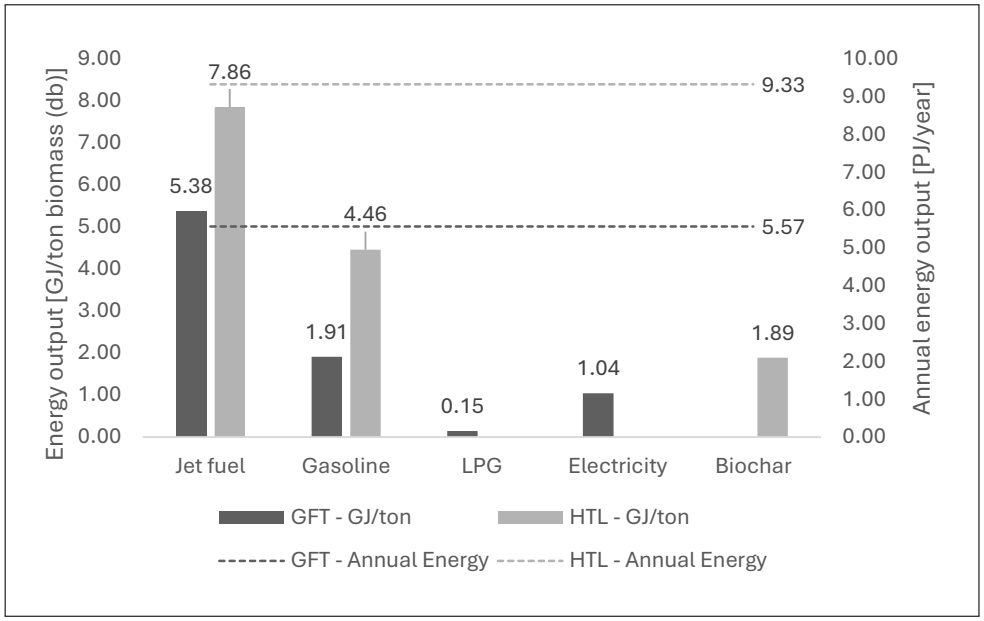

Fig. 4. Energy Yield per Product for GFT and HTL Pathways

by a factor known as the learning rate (LR), defined in Equation 3. **Merrow** [53] provide a formulation specific to chemical processes, as shown in Equation 4.

$$PR = 2^{b} \tag{2}$$

$$LR = 1 - PR = 1 - 2^{-b} \tag{3}$$

$$\begin{aligned} PR = {} & 92.3 - 3.2\% \times \text{number of (thermo)-chemical processes} \\ & + 6.5\% \quad \text{if main process involves solids} \\ & + 5.0\% \quad \text{if product is a primary chemical} \\ & + 5.0\% \quad \text{if the product is a liquid} \end{aligned} \tag{4}$$

The assumptions and results for technological learning are summarized in Table 5. As gasification and hydrothermal liquefaction are considered the main processes and involve solid feedstocks, this is accounted for in the learning curve equation. **Merrow** [53] defines a "primary chemical" as a product not derived from a feedstock that is itself a chemical product. In this study, forestry residues are used as feedstock; since they are not a chemical product, this condition is met and incorporated into the equation. For both processes, the final products are liquids (primarily SAF and gasoline), which is also reflected in the calculation.

For the GFT pathway, the following (thermo)-chemical processes are considered: indirectly heated gasifier (*Block 4*), tar reformer (*Block 5*), steam reformer and WGS (*Block 8*), LTFT (*Block 10*), alkylation & oligomerization (*Block 11D*), aromatization (*Block 11E*), hydrocracker (*Block 11F*), and hydrotreater (*Block 11I*). For the HTL pathway, the considered processes include: HTL reactor (*Block 3*), anaerobic digestion (*Block 8*), hydrogen plant (*Block 9*), hydrodeoxygenation (*Block 7A*), dehydrogenation (*Block 7D*), oligomerization (*Block 7E*), hydrogenation (*Block 7F*), isomerization (*Block 7G*). The numbers in parentheses refer to the corresponding unit process blocks in Figure 3.

Table 5. Assumptions for technological learning applied for the GFT and HTL pathways.

	GFT	**HTL**
P_0	7[a]	6[a]
P_t	121[b]	121[b]
Number of (thermo)-chemical processes	8	8
+ 6.5% if main process involves solids	Yes	Yes
+ 5.0% if product is a primary chemical	Yes	Yes
+ 5.0% if the product is a liquid	Yes	Yes
Learning rate (LR)	16.8%	16.8%
Technology Learning Factor (TLF) $= (\frac{P_t}{P_0})^{-b}$	0.469	0.451

[a] [52], assuming 5% market penetration [b] [10]

The resulting learning rate (Table 5) for both the GFT and HTL pathways is similar at 16.8%. However, since fewer HTL facilities have been installed (P_0), the resulting Technological Learning Factor (TLF) is slightly lower for HTL (0.451) than GFT (0.469), giving it a greater impact on the reduction of TCI. Historical learning rates for these thermochemical pathways, which include both the thermochemical conversion process and the SAF refinery, are not available due to the lack of data. However, a comparison with other technologies is possible. **Hettinga et al.**, **Cavalett et al.**, and **Van den Wall Bake et al.** [54, 55, 56] reported learning rates of 18% and 19% for corn ethanol production in the United States and Brazil, respectively. **Merrow** [53] analyzed more than 40 chemical processes and found an average learning rate of 20%. Using a similar methodology, **Weber et al.** [57] reported a learning rate of 23% for HTL with electrochemical upgrading of bio-oil.

4.2.2 Operational Expenditures

Annual OpEx are divided into two categories: fixed operating costs and variable operating costs. Fixed operating costs remain constant regardless of production capacity, whereas variable operating costs vary directly with production levels. The calculation of OpEx follows the methodology outlined by **Seider et al.** [58].

The assumptions and parameters for fixed operating expenses are provided in Table 6. These costs include:

- Labor-related expenses: dependent on Direct Wages & Benefits (DW&B). An estimation is made on number of operators per process section based on type of processes; continuous or batch operation and state of flows (fluids/gas, solids-fluids, solids).
- Maintenance expenses: dependent on Maintenance Wages & Benefits (MW&B). Depending on the the state of flows (fluids/gas, solids-fluids, solids) per process section, a specific portion of Total Depreciable Capital (TDC) is allocated to the MW&B.
- Operating overhead: dependent on M&O-SW&B[1].
- Insurance: dependent on TDC.
- Local taxes: dependent on TDC.

The variable costs are primarily determined by the utility profile presented in Table 3. Price levels for utilities are adjusted to 2024 values using regional inflation factors corresponding to the source location of each price. Further details on the applied price levels are provided in Appendix A.

4.2.3 Capital Expenditures

Capital expenditure is determined by aggregating the component costs for all unit process blocks, including installation. Original equipment costs, obtained from literature and APEA (Figure 1), are adjusted for the installation year using the Chemical Engineering Plant Cost Index (CEPCI), plant scale using a capacity scaling exponent n, and installed cost using an installation factor (IF_i) for each component i.

$$C_{\mathrm{inst.},i} = C_{\mathrm{base},i} \times \frac{\mathrm{CEPCI}_{\mathrm{new},i}}{\mathrm{CEPCI}_{\mathrm{base},i}} \times \left(\frac{Q_{\mathrm{new},i}}{Q_{\mathrm{base},i}}\right)^{n} \times \mathrm{IF}_i \quad (5)$$

Here, $C_{\mathrm{inst.},i}$ is the installed cost in the installation year at the adjusted scale. $C_{\mathrm{base},i}$ is the reported base-year cost at its base scale $Q_{\mathrm{base},i}$, and $Q_{\mathrm{new},i}$ is the target scale in the current design. IF_i is the installation factor. $\mathrm{CEPCI}_{\mathrm{base},i}$ and $\mathrm{CEPCI}_{\mathrm{new},i}$ denote the CEPCI values for the base and installation years, respectively, for component i.

Using this CapEx data, the Total Capital Investment (TCI) can be determined. TCI represents the upfront costs incurred before and during plant construction and comprises several components detailed in Table 6.

The TCI consists of five cost components. First, the Total Installed Cost (TIC) includes all equipment costs once installed (Equation 5). Second, indirect costs (IC) cover expenses not directly related to equipment, such as engineering, plant design, construction, and associated services. Third, a Technological Learning Factor (TLF), described in Section Technological Learning, is applied. Fourth, a location correction factor is applied, as the original cost data were sourced from projects in the United States. Finally, working capital accounts for the funds required for day-to-day operations after commissioning. Together, these components yield the TCI. The final values are reported in Table 7: €230.0 M for GFT and €303.4 M for HTL, both including CO_2 capture modules.

4.2.4 Discounted Cash Flow Rate of Return

The Discounted Cash Flow Rate of Return (DCFRR) methodology is widely applied to assess the economic feasibility of a project by incorporating all associated costs and revenues over its lifetime, while accounting for the internal rate of return (IRR) [14, 59, 18]. Financial parameters for DCFRR method are outlined in Table 6. Earnings depend on the price level of sustainable aviation fuel (SAF), which can vary over time and introduce uncertainty into the analysis. To more robustly determine economic viability, it is preferable to calculate the minimum fuel selling price (MFSP) at which the project breaks even over its lifetime for a specified IRR. This is achieved by setting the Net Present Value (NPV) of the cash flows to zero, as shown in the following equation:

$$\mathrm{NPV} = \sum_{t=-2}^{0} \frac{-C_{\mathrm{TCI},t}}{(1+r)^t} + \sum_{t=1}^{n} \frac{C_t}{(1+r)^t} = 0 \quad (6)$$

Here, $C_{\mathrm{TCI},t}$ is the capital investment in year t (negative cash flows), C_t is the net annual cash flow in year t, r is the internal rate of return, and n is the project lifetime in years. *Goal Seek* analysis tool in Microsoft Excel® is used, which makes use of the Newton-Raphson root finding method [62].

Depreciation of the components is calculated using the Modified Accelerated Cost Recovery System (MACRS). This method allocates a greater portion of depreciation to the early years of the project, thereby reducing taxable income during these periods. Consequently, higher cash flows are realized in the initial years, when their effect on the discounted cash flow is more significant, which in turn increases the project's Net Present Value (NPV) [58].

4.2.5 Economic Performance

Table 7 presents the final cost break down results. OpEx is divided into fixed and variable costs, as well as variable operating income from byproduct sales. CapEx are shown as costs per key plant section in total installed cost (TIC) and as total capital investment (TCI). The minimum fuel selling price (MFSP) is also reported. For both TCI and MFSP, values are provided with and without the inclusion of technological learning rates (TLR). The full economic breakdown is presented for scenarios both including and excluding CO_2 capture.

[1] M&O-SW&B = DW&B + MW&B + MS&B

Table 6. Fixed operating expenses, total capital investment and financial model parameters. Values that are identical for both GFT and HTL are centered across the two columns, while parameters with different values are listed in their respective columns.

Parameter	Unit	Value (GFT)	Value (HTL)	Reference
Labor-related expenses				
Direct wages and benefits (DW&B)				
Number of operators per shift		14	10	[58]: Tab. 23.3
Shifts	#	5		[58]: Pag. 610
Hours per year	h	2080		[58]: Pag. 610
Wage and benefits operator (incl taxes)	€/h	42.92		–
Operating supplies and services	% of DW&B	6.0%		[58]: Tab. 23.1
Technical assistance to manufacturing	% of DW&B	14.0%		[58]: Ex 23.8
Control laboratory	% of DW&B	15.0%		[58]: Ex 23.8
Maintenance Expenses				
Total Depreciable Capital (TDC)	–	= TDIC		[58]: Tab. 22.9
Wages and benefits (MW&B)	% of TDC	3.5-5%[a]	3.5-5%[a]	[58]: Tab. 23.1
Salaries and benefits (MS&B)	% of MW&B	25.0%		[58]: Tab. 23.1
Materials and services	% of MW&B	100.0%		[58]: Tab. 23.1
Maintenance overhead	% of MW&B	5.0%		[58]: Tab. 23.1
Operating Overhead, Insurance, and Local Taxes				
Operating overhead	% of M&O-SW&B	22.8%		[58]: Tab. 23.1
Insurance	% of TDC	1.0%		[58]: Pag. 612
Local taxes	% of TDC	3.0%		[58]: Pag. 612
Total Installed Cost (TIC)	–	$\sum_i C_{\text{installation},i}$		–
Total Purchase Equipment Cost (TPEC)	–	$\sum_i C_{\text{installation},i}$ (excl. IF)		–
Indirect Costs (IC)	% of TPEC	132.0%		[14]: Tab. 2-2
Engineering	% of TPEC	32.0%		[14]: Tab. 2-2
Construction	% of TPEC	34.0%		[14]: Tab. 2-2
Legal and Contractors Fees	% of TPEC	23.0%		[14]: Tab. 2-2
Project Contingency	% of TPEC	37.0%		[14]: Tab. 2-2
Land purchase	% of TPEC	6.0%		[59]: Tab. 9
Location Factor (US to NL)	% of TDIC	23.0%		[60]
Total Direct and Indirect Cost (TDIC)	–	$(\text{TIC} + \text{IC}) \times \text{TLF} \times (1 + \text{LF})$		–
Working Capital (WC)	% of TDIC	15.0%		[59]: Tab. 9
Total Capital Investment	–	$\text{TDIC} \times (1 + \text{WC})$		–
Plant financing				
Equity / Debt ratio	% of TCI	40% / 60%		[38]
Loan interest	%	8%		[38]
Payback period	y	10 (annuity loan)		[38]
Depreciation period	y	7-10[a]	7-20[a]	[58]: Tab. 23.10
Construction period				
Construction period	y	3		[59]
% spent in year $-2, -1, 0$	%	8%, 60%, 32%		[59]
Startup time and ramp-up				
Startup time	y	0.50		[59]
Revenues	%	50%		[59]
Fixed operating costs	%	100%		[59]
Variable operating costs	%	50%		–
Other financial parameters				
Internal rate of return (after taxes)	%	10%		[59]
Income tax rate	%	25.8%		[61]
Plant life time	y	20		[59]

[a] depends on specific process component, see Appendix A.

Table 7. Cost break down for Gasification Fischer-Tropsch and Hydrothermal Liquefaction in €M.

	GFT		HTL	
	CO_2	**Non-CO_2**	**CO_2**	**Non-CO_2**
Fixed Operating Costs	40.3	37.2 (-8%)	45.6	44.9 (-1%)
Feedstock	37.3	37.3	37.3	37.3
Water	2.2	2.2	0.1	0.1
Electricity (consumption)	37.8	37.2	28.7	28.5
Natural gas	18.4	18.4	–	–
Olivine	1.7	1.7	–	–
Hydrogen	0.6	0.6	3.6	3.6
Steam	14.1	14.1	0.4	0.4
Catalysts + Chemicals	2.5	2.4	11.2	11.2
WWT + Ash disposal	1.9	1.9	1.3	1.3
CO_2 transport and storage costs	17.7	–	4.7	–
Variable Operating Costs	134.0	115.7 (-14%)	87.4	82.5 (-6%)
CO_2	49.8	–	13.3	–
Char	–	–	9.0	9.0
Gasoline	22.9	22.9	53.5	53.5
LPG	3.2	3.2	–	–
Electricity (production)	33.3	33.3	–	–
Variable Operating Income	109.3	59.4 (-46%)	75.8	62.5 (-17%)
Operating profit (excl. SAF sales)	-65.1	-93.5	-57.1	-64.9
Pretreatment (*Block: 2-3 | 2*)	14%	16%	26%	26%
General Plant (*Block: 4-10 | 3-6*)	53%	59%	22%	22%
SAF Refinery (*Block: 11 | 7*)	7%	8%	26%	27%
Steam generation plant (*Block: 12 |*)	15%	17%	–	–
Anaerobic digestion plant (*Block: | 8*)	–	–	9%	10%
Hydrogen plant (*Block: | 9*)	–	–	14%	15%
CO_2 capture modules (*Block: 13 | 10*)	10%	0%	2%	0%
Total Installed Cost (TIC)	100%	100%	100%	100%
Total Direct and Indirect Cost (TDIC)	200.0	179.8 (-10%)	263.8	258.5 (-2%)
Total Capital Investment (TCI) (excl. TLF)	489.9	440.5	673.3	659.8
MFSP [€/L] (excl. TLF)	2.56	2.84 (+11%)	2.05	2.10 (+3%)
Total Capital Investment (TCI)	230.0	206.8	303.4	297.3
MFSP [€/L]	1.49	1.87 (+26%)	1.03	1.10 (+7%)

Fixed operating costs for GFT (€40.3 M) are 12% lower than for HTL (€45.6 M), despite higher labor expenses due to a larger number of operators per shift. This is primarily the result of significantly lower maintenance costs, which are directly linked to the total direct investment cost (TDIC). When CO_2 capture modules are excluded, fixed OpEx decreases more sharply for GFT (–8%) than for HTL (–1%), reflecting the larger CapEx share of CO_2 capture modules in GFT (10%) compared to HTL (2%).

Variable operating costs for GFT (€134.0 M) are 53% higher than for HTL (€87.5 M). GFT exhibits higher utility costs across all categories except “Catalysts & Chemicals” and ”Hydrogen”. The higher ”CO_2 transport and storage costs” for GFT are due to the larger volume of CO_2 captured. As expected, when CO_2 capture modules are excluded, GFT costs decrease more sharply than HTL (–14% vs –6%). This reduction results from the removal of costs associated with electricity, amine usage (Catalysts & Chemicals), and CO_2 transport and storage.

Variable operating income represents revenue from the sale of byproducts. GFT generates 44% higher income than HTL, primarily due to the substantial contribution from CO_2 credits (€49.8 M) sold under the EU ETS scheme [26]. Although net electricity production is positive, the re-

sulting income (€33.3 M) is lower than the corresponding cost (€37.8 M) because the selling price of electricity is lower than the purchase price [2]. Additional revenue streams for GFT include gasoline (€22.9 M) and LPG (€3.2 M). For HTL, the largest contributor is gasoline sales (€53.5 M), supplemented by smaller revenues from CO_2 credits (€13.3 M) and biochar (€9.0 M). When CO_2 capture modules are excluded, GFT's income decreases significantly (–46%) compared to HTL (–17%).

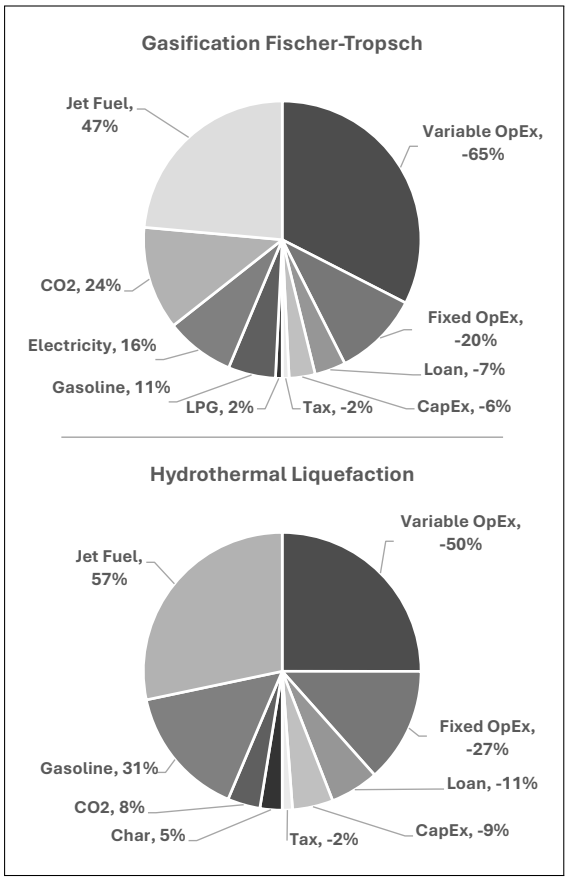

Fig. 5. Contribution of each cost component where positive percentages account for income, and negative percentages account for costs.

The CapEx results are broken down into key process sections and their contributions to the TIC, with percentage shares identical to those in the TCI. For GFT, the largest contributor is the general plant section (53% & 59%), due to the large number of unit processes included in this section and intense operating conditions for these processes. For example, the gasification reactor operates at high temperature (870∘C) and the syngas after compression (*Block 7-10*) operates at high pressures (31 bar). In contrast, HTL shows a more balanced distribution across process sections, with pretreatment representing a notable 26% share. This high contribution is primarily due to the feed/product exchanger, which heats the slurry using energy recovered from the reactor effluent (Appendix A). This results from a high mass flow, due to significant water content to form the slurry, medium temperatures (300∘C), and extreme high pressures (205 bar). Consistent with previous findings, the contribution of CO_2 capture modules has a greater impact on the GFT pathway (–10%) than on HTL (–2%). This difference arises because GFT requires two extra capture modules and operates at a larger scale. Additionally, GFT's generally lower overall CapEx results in a proportionally higher contribution from the CO_2 capture module costs. The Total Direct Investment Cost (TDIC) changes follow the same trend.

The TCI for GFT (€230.0 M) is 24% lower than that for HTL (€303.4 M); however, the reported MFSP is 31% lower for HTL (€1.03/L) than for GFT (€1.49/L). Two key factors explain the lower MFSP for HTL. First, the operating profit (excluding SAF sales) is higher, or less negative, for HTL than for GFT (€–57.1 M vs €–65.1 M). Second, as shown in Table 4, the SAF output of HTL is approximately 47% higher than that of GFT, allowing for a lower selling price despite the higher TCI. Consistent with other financial parameters, CO_2 capture modules have a greater impact on the MFSP for GFT than for HTL (+26% vs +7%).

Interestingly, when technological learning is not accounted for, the TCI and MFSP for both thermochemical pathways increase substantially. According to Table 7 for the inclusion of CO_2 capture modules, the negative change in MFSP of HTL when including TLF is almost halfed, 99%, while GFT decreases by 72%. The sensitivity of MFSP to the exclusion of CO_2 capture modules is lower when the technological learning factor (TLF) is included (GFT: +26%, HTL: +7%) compared to when it is excluded (GFT: +11%, HTL: +3%). This can be explained by the fact that a higher TCI results in a greater contribution of capital costs to the MFSP, thereby reducing the relative impact of higher operating profits from CO_2 credits.

Figure 5 shows the contribution of each cost and income component to the MFSP (including CO_2 capture modules). On the income side, GFT exhibits a more diverse distribution of (by)product sales compared to HTL with the two biggest contributors accounting for 88% for HTL and only 71% only for GFT. On the cost side, variable OpEx has a larger share for GFT than for HTL, which corresponds with the results in Table 7. This also corresponds with the contribution of feedstock costs to the MFSP, where the contribution is lower for GFT (28% of variable OpEx) than for HTL (43% of variable OpEx). In contrast, CapEx and loan costs are higher for HTL (9% & 11%), consistent with Table 7, as the TCI for HTL exceeds that of GFT (€303.4 M vs €230.0 M).

4.3 Sensitivity Analysis

Figure 6 give the result of the sensitivity analysis for GFT and HTL (including CO_2 capture modules). On the y-axis the different parameters are outlined with the change of the parameter in parantheses. On the x-axis the absolute change in MFSP is outlined where the bars on the left indicate the negative change in MFSP (cheaper MFSP)

[2] An overview of utility price levels is given in the spreadsheet model Appendix A

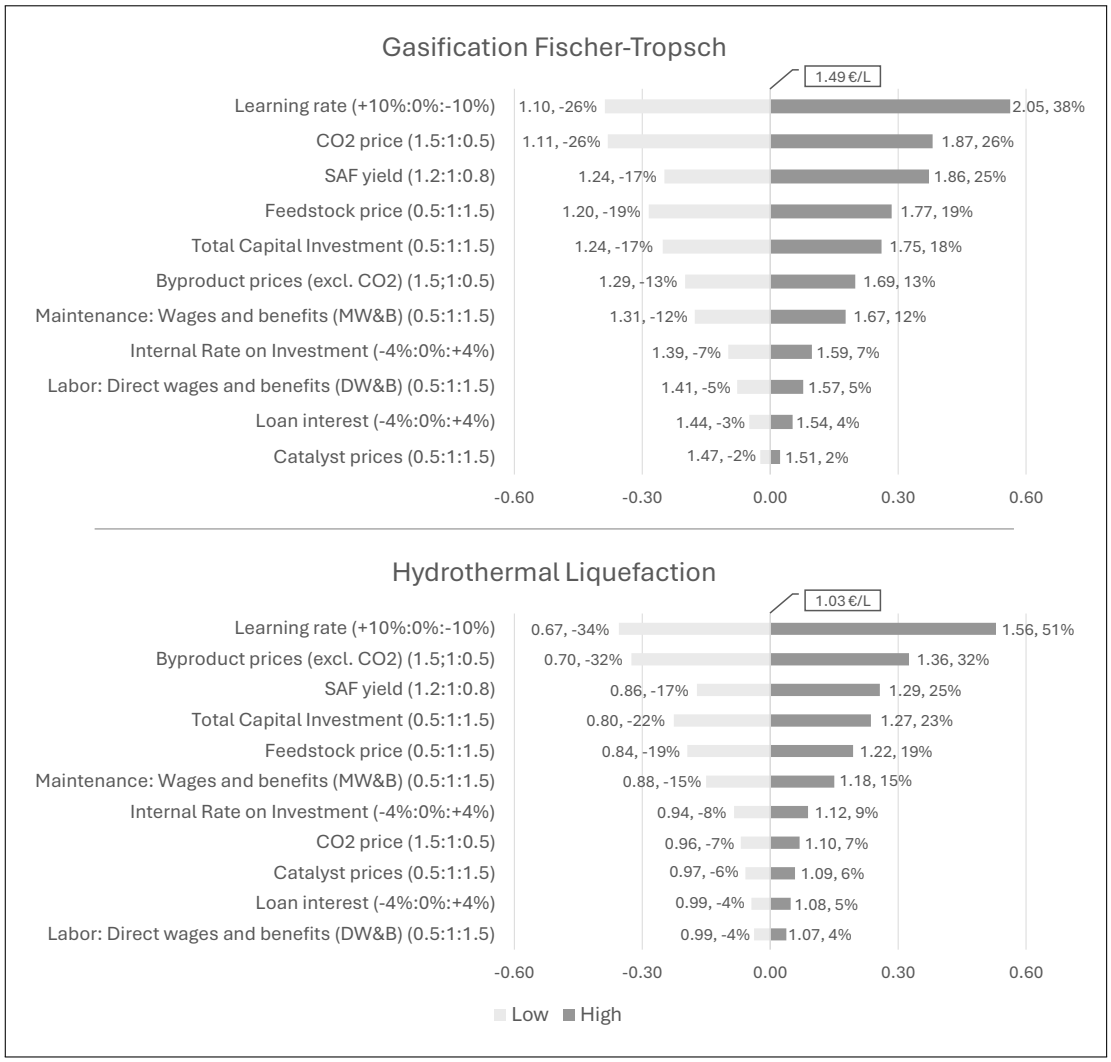

Fig. 6. Sensitivity Analysis for Gasification Fischer-Tropsch and Hydrothermal Liquefaction.

and the bars on the right indicate the positive change in MFSP (more expensive MFSP). The numbers next to the bars indicate the new MFSP under these conditions, while the percentage indicated the relative change in percentage. This relative change is convenient when comparing GFT and HTL as due to different base MFSP absolute changes only show part of the sensitivity.

Both technologies are highly sensitive to the learning rate, and the observed asymmetric behavior can be explained by the exponential form of the learning curve Equation 3, which introduces non-linearity. As a result, increases in the learning rate lead to disproportionately stronger reductions in MFSP, while decreases in the learning rate cause comparatively weaker increases. SAF yield also shows a disproportionate relationship, as the relative increase becomes stronger due to the reciprocal nature of the MFSP calculation. Since MFSP is defined as the ratio of costs to output, keeping costs constant while increasing SAF yield results in a non-linear reduction of MFSP. Although not directly visible in the GFT graph, the internal rate of return (IRR) also follows a non-linear relationship, as shown in Equation 6. Loan interest payments are calculated using an annuity loan structure, where repayments remain constant over the payback period. This calculation also follows a non-linear function. The same reasoning explains the disproportionate behavior observed in the total capital investment (TCI): higher TCI increases the loan amount, which in turn raises loan payments, thereby reinforcing the non-linear effect.

The sensitivity analysis confirm some previous findings both for GFT and HTL. According to Table 7, it was found that the negative change in MFSP of HTL when including TLF is almost halfed, 99%, while GFT decreases by 72%. The sensitity analysis shows a similar behaviour where HTL is more sensative than GFT when looking at the relative change in MFSP due to learning rate changes (HTL:-34% & 51% vs GFT:-26% & 38%).

As expected the MFSP of GFT is more sensitive than HTL for changes in CO_2 price, underscoring its dependency on this byproduct. On the other hand HTL is more sensitive to byproduct prices (excluding CO_2 prices) as a great amount of MFSP contribution comes from byproducts (Figure 5)

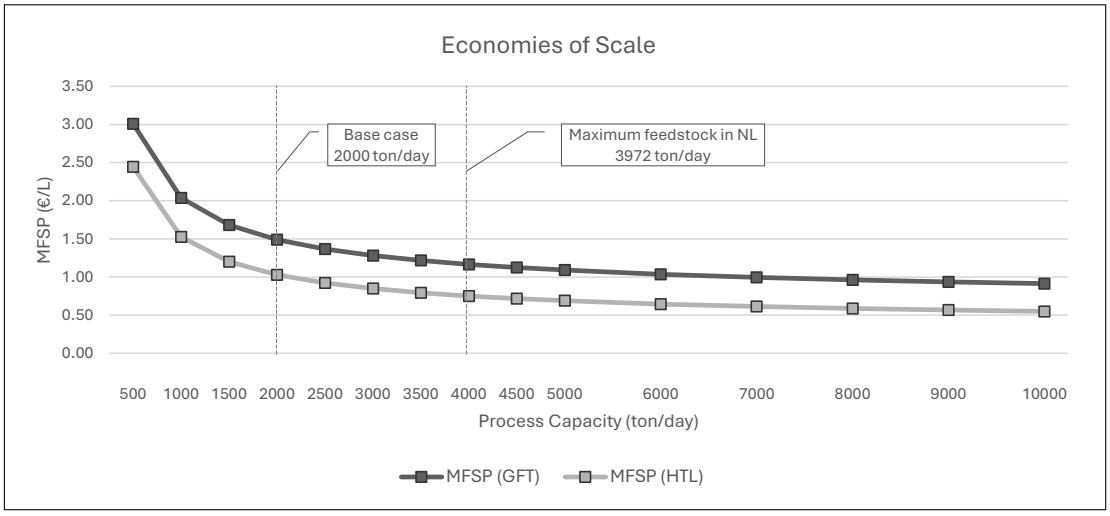

Fig. 7. Economies of scale for Gasification Fischer-Tropsch and Hydrothermal Liquefaction.

Figure 7 shows the MFSP against the process capacity in t_{db}/d. The process capacity of the base case is 2000 t_{db}/d whereas the maximum capacity when considering Dutch forestry residue is 3972 t_{db}/d [28]. Going over that limit means buying feedstock abroad which increases the price due to transportation costs. The graph shows an economic of scale behaviour where the MFSP decreases as process capacity increases. This can be explained as CapEx scale disproportionally when capacity is increased do to scale factor, n (Equation 5), which gives it a non-linear behaviour. This also affects the fixed costs that as an effect also scale disproportionally. Variable costs scale linearly.

4.4 Scenario Analysis

The technical and economic comparison between GFT and HTL reflects only the base case analysis, while the sensitivity analysis evaluates the effect of changing a single parameter at a time. To better capture potential variations in MFSP, a scenario analysis is performed for both a conservative and a progressive case, each including CO_2 capture modules. The parameter deviations are aligned with those used in the sensitivity analysis to ensure consistency and traceability.

The conservative scenario assumes a disappointing learning rate ($\Delta =$ -10%) due to slow technology deployment, limiting experience in large-scale operations. Learning rate is now in line with more conservative studies [63]. As a result, capital costs (TCI) are not expected to decrease significantly. In addition, feedstock prices are assumed to rise ($\Delta = \times 1.5$), which could result from increasing competition for renewable biomass in the coming decades. Labor costs are also expected to increase ($\Delta = \times 1.5$), as the Netherlands faces a persistent labor shortage and specialized chemical plant operators are projected to become scarce [64, 65].

The progressive scenario, by contrast, assumes that byproducts can be sold at higher prices due to market premiums compared to their fossil-based counterparts ($\Delta = \times 1.5$). The Netherlands has already introduced HBE (Renewable Fuel Units) certificates, which can be traded in a manner similar to CO_2 credits; a surplus of these certificates can be sold on the market [67]. Loan interest for renewable projects could be reduced to incentivize investment in decarbonization, or airlines may provide capital support to secure SAF supply ($\Delta =$ -4%). Furthermore, technological advancements are assumed to improve SAF yields for both thermochemical pathways ($\Delta = \times 1.2$).

A summary of the scenarios and corresponding impact on parameters:

- **Conservative scenario**: learning rate ($\Delta =$ -10%), feedstock price ($\Delta = \times 1.5$), direct wages & benefits (DW&B, $\Delta = \times 1.5$);
- **Progressive scenario**: byproduct price ($\Delta = \times 1.5$), loan interest ($\Delta =$ -4%), SAF yield ($\Delta = \times 1.2$);
- **Both scenarios**: effects of CO_2 price are considered at 0.5× and 1.5× the base value. Base value is €60/t.

The results of the scenario analysis are presented in Figure 8. A maximum process capacity of 3,500 t_{db}/d is shown, reflecting feedstock constraints in the Netherlands (Figure 7). CO_2 price fluctuations is indicated by the error bars, where the higher CO_2 price leads to a lower MFSP and vice versa. GFT exhibits an MFSP range of €0.82–3.28/L, while HTL ranges from €0.36–2.59/L. The conservative scenario has a stronger impact on MFSP, partly because learning rate and feedstock price were identified as highly sensitive parameters in Figure 6.

The colored circles in red, orange, and green indicate different levels of economic feasibility. The red circle represents price competitiveness with the current HEFA price (€1.67/L) under a conservative scenario. The HEFA pathway is currently the lowest-cost SAF option, while data for SAF from advanced feedstocks such as forestry residues remain unavailable. For GFT, competitiveness with HEFA is achieved only under optimum conditions, namely at high CO_2 prices and large process capacities (3500 t_{db}/d). For HTL, competitiveness is already reached at a process ca-

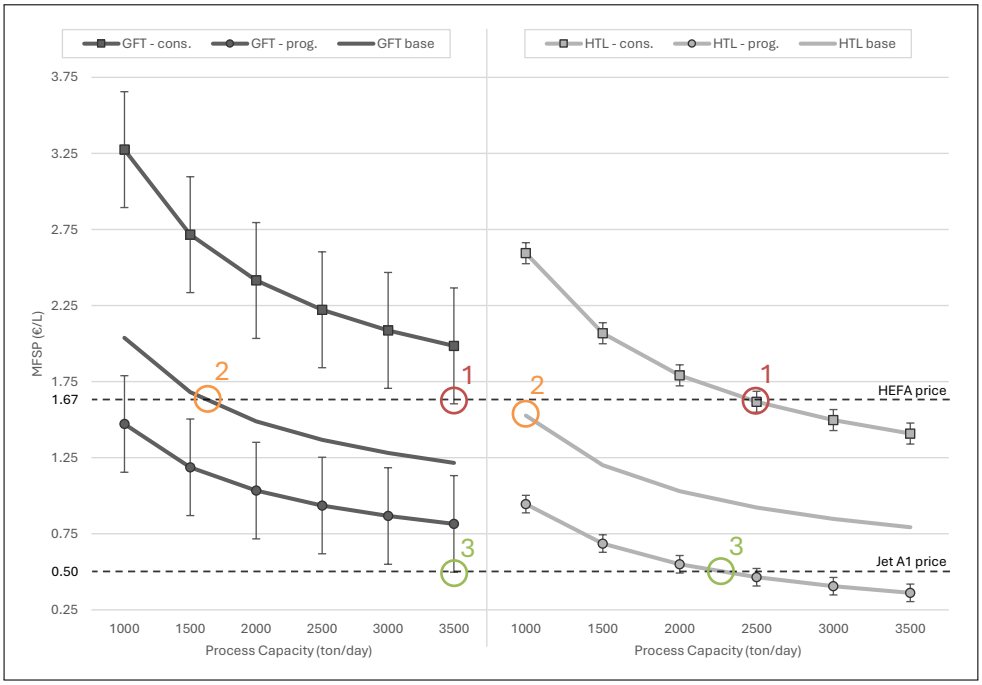

Fig. 8. Conservative, progressive, and base scenarios for GFT (left) and HTL (right), showing MFSP across process capacities. Error bars represent CO_2 price variations (0.5× and 1.5×). Market prices of Jet A1 (fossil kerosene) and HEFA are included for comparison [30, 66]. The three colored circles indicate different levels of economic feasibility.

pacity of 2,500 t_{db}/d, and CO_2 price fluctuations have only a limited effect on the MFSP.

The orange circle indicates the competitiveness of the base case scenario with HEFA. For GFT, a comparable price of €1.67/L is achieved at a significantly lower process capacity of approximately ±1,600 t_{db}/d. Under these base conditions, economic feasibility improves due to reduced dependence on large quantities of feedstock. At the highest process capacity (3,500 t_{db}/d) a price discount of 27% is achieved, while feedstock dependency is highest. For HTL, a price discount of 8% compared to HEFA is already obtained at 1,000 t_{db}/d, and competitiveness improves further with increasing process capacity, reaching a discount of 53% at the maximum capacity.

The green circle represents the most notable level of feasibility, indicating competitiveness with fossil jet fuel (Jet A1, priced at €0.50/L) under a progressive scenario. Achieving competitiveness at this benchmark is significant, as the aviation industry remains 99.7% dependent on fossil kerosene [3]. For GFT, competitiveness is reached only at high CO_2 prices and large process capacities, and even then no price discount is realized, with the MFSP remaining at €0.50/L. In contrast, HTL achieves price competitiveness from a process capacity of ±2,250 t_{db}/d. At 2,500, 3,000, and 3,500 t_{db}/d, HTL reaches price discounts of 8%, 18%, and 28%, respectively. These results highlight HTL as a strong candidate for replacing fossil jet fuel under progressive conditions in 2050. However, this outlook is definitive only if technological learning is realized by installing a sufficient number of plants ($P_t = 121$, subsubsection 4.2.1) by 2050.

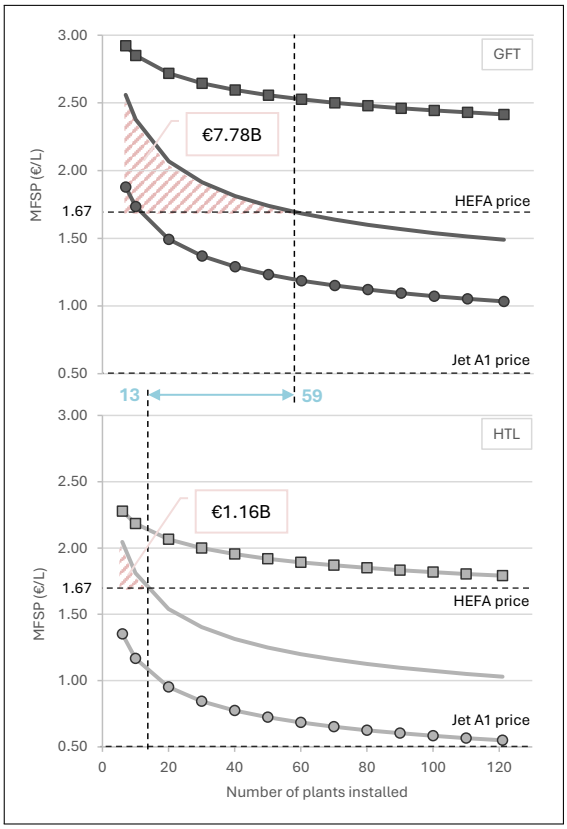

Fig. 9. Impact of the number of globally installed plants on the MFSP, with an indication of the subsidies required to incentivize industry deployment. GFT is shown at the top and HTL at the bottom. Process capacity is fixed at 2000 t_{db}/d.

To analyze this, Figure 9 shows the effect of the number of installed plants on the MFSP. The three scenarios are presented in the same style as Figure 8 for GFT (top) and HTL (bottom), alongside benchmark prices for Jet A1 and HEFA. As expected, increasing the number of plants reduces the MFSP, since each new installation adds to cumulative experience. Notably, HTL achieves competitiveness with HEFA with as few as 13 globally installed plants, whereas GFT requires 59 plants to reach the same price level. This indicates that the economic feasibility of HTL plants is likely to be achieved before 2050, under the assumption of a definitive $P_t = 121$ in 2050. The red area represents the total subsidies required on capital investment (TCI) to reduce the MFSP to the level of the HEFA price. This provides an indication of the scale of global governmental support needed to incentivize fuel producers by making early-stage plants cost competitive. HTL requires nearly seven times less subsidy than GFT, with estimated needs of €1.16 B for HTL compared to €7.78 B for GFT.

4.5 Uncertainty Analysis

A Pedigree Analysis was conducted to assess the strengths, weaknesses, and uncertainties of the data used as input for the technical and economic model, as well as uncertainties inherent in the model itself [68]. The assessment was carried out by the researcher, the supervisor, and an external expert. Each section of the model was evaluated on four criteria:

- *Proxy*, refers to how good or close a measure of the quantity that we model is to the actual quantity we represent
- *Emperical basis*, refers to the degree to which direct observations, measurements and statistics are used to estimate the parameter.
- *Theoretical understanding*, measures the degree of theoretical understanding that was used to generate the numeral of that parameter.
- *Methodological rigor*, refers to the norms for methodological rigor in this process applied by peers in the relevant disciplines.

Scores were assigned on a scale from 0 (lowest) to 4 (highest). The resulting matrices are presented in the Appendix B. The main weaknesses identified are summarized below:

- Empirical basis received the lowest scores (2.00-2.67; average of 2.28), as most data were derived from Aspen Plus® simulations, representing indirect rather than direct measurements. In addition, some data were obtained from papers and reports considered old, though not outdated.
- The energy balance for GFT was not directly sourced from a foundational study but instead calculated by the researcher. Although this approach is common, most technical models in literature rely on data that is self-developed Aspen Plus® simulations to obtain energy balances.
- HTL CapEx data were primarily obtained from indirect sources, as no direct foundational paper was available. This led to lower scores for both empirical basis and proxy.
- Fixed operating costs were estimated using methods commonly found in literature; however, this category was still judged to be a rule-of-thumb approximation.
- Technological learning was calculated using approaches described in literature, but only limited sources were available. Consequently, the estimates relied largely on rule-of-thumb assumptions and could not be considered common practice.

5 Discussion

Several findings from the Pedigree Analysis require further discussion. Regarding the first point on the use of older data, this limitation is partly mitigated by design improvements performed on the process data used from literature. These included the integration of CO_2 capture modules, the use of recent catalyst data, and the proposal of updated refinery designs for SAF production. However, key process variables related to reaction yields, such as biomass-to-syngas and syngas-to-syncrude yields for GFT, and biomass-to-biocrude yield for HTL, still rely on older experimental data. On the other hand, according to the Pedigree Analysis the proxy, theoretical understanding and methodological rigor scored sufficient showing confidence in the data that is used.

Although the learning rate was calculated using well-defined methodologies and comparable technologies have demonstrated high technological learning percentages (18-23%), it remains a highly uncertain parameter. More conservative studies, such as those from the National Energy Technology Laboratory (NETL) in the United States, recommend using learning rates of 6% for novel technologies [63]. Due to this uncertainty, methodological rigor only barely achieves a sufficient score (2.50). Furthermore, the high sensitivity observed in Figure 6 makes it difficult to draw firm conclusions regarding the MFSP. Another concern is the direct dependency of fixed operating costs on the TCI. When TCI decreases as a result of technological learning, fixed costs also decrease, which may not fully reflect real-world conditions. This is underpinned by the proxy that marginally meets a sufficient score (2.50).

A further limitation is that the SAF refinery model did not include catalyst consumption. Since the GFT refinery was modeled as a single unit process block, individual mass flows between the different chemical reactions were not available. Without this information, estimating catalyst consumption would have been highly uncertain. For consistency, catalyst consumption for HTL was also not considered. By not including this SAF refinery catalyst consumption an incomplete representation of the MFSP is given.

The economic model relies on price levels available for 2024 but forecasts production costs of SAF in 2050. Since

price levels for 2050 cannot be reliably estimated, this introduces an inherent uncertainty that must be considered. This is underscored in the Pedigree Analysis where variable operating costs resulting a score of 2.50, just meeting the sufficient score. On the other hand, over time more reliable data will be available for price levels, and can subsequently be implemented in this model. Similarly, the comparison of MFSP with HEFA prices is based on current HEFA values, as no future projections are available in the literature. On the other hand, HEFA prices are strongly dependent on feedstock costs, and the pathway requires relatively little capital investment. As a result, learning rates are expected to have limited impact on HEFA production costs, which may remain relatively stable or even increase in the future due to rising feedstock demand and prices [69].

Another limitation concerns the project lifetime, which was set at 20 years without accounting for the residual value of the chemical plant. While this assumption is consistent with the methodology of several previous studies, it may underestimate the actual lifetime of most plants, which often exceed 20 years [70]. Accounting for a longer operating lifetime or including residual value would reduce the MFSP.

When considering this SAF production plant in 2050, a significant share of available feedstock in the Netherlands would need to be redirected toward SAF production. A potential price increase resulting from this additional demand was not included in the analysis, which may further affect the economic outcomes.

6 Conclusion

This study evaluated the techno-economic feasibility of two thermochemical pathways for converting Dutch forestry residues into SAF through a side-by-side comparison of process designs, mass and energy balances, and cost structures, with the objective of maximizing SAF production. The system design incorporates CO_2 capture and storage to improve environmental performance, and technological learning rates are included to project pathway performance in 2050.

In terms of SAF yield, HTL proved to be the stronger pathway with a 47% higher yield than GFT (18.3% vs 12.5%). HTL also produced higher yields of gasoline and biochar, whereas GFT generated lower gasoline output along with some LPG. GFT was superior in CO_2 production, with a yield of 127.4% compared to 33.9% for HTL. With CO_2 capture, GFT showed a better environmental performance than HTL, being almost carbon negative in its operation with a carbon efficiency of 96.8%. Also waste generation under CO_2 capture GFT benefits the most having a more enviromental E-factor. HTL demonstrated 68% higher performance in terms of annual energy output for all its (by)products, delivering 9.33 PJ/year compared to 5.57 PJ/year for GFT.

In terms of economic performance, HTL also proved to be the stronger pathway, despite its higher total capital investment. Technological learning factors were slightly more favorable for HTL, due to the smaller number of currently installed FOAK plants. The resulting MFSP was €1.03/L for HTL and €1.49/L for GFT. The main contributors to HTL's advantage are its higher operating profit (excluding SAF sales) and greater SAF yield. Compared to HEFA (€1.67/L), HTL shows a 38% discount versus 11% for GFT. Since HEFA already has established demand at this price level, SAF from HTL and GFT could be positioned as the least expensive renewable kerosene alternative.

The MFSP values obtained for both HTL and GFT fall within the lower range of values reported in the literature. However, previous studies generally did not incorporate technological learning or CO_2 capture, which would likely have resulted in lower MFSP values. Notably, literature findings also consistently reported lower MFSP for HTL compared to GFT, further supporting HTL's superior economic performance.

The scenario analysis showed that GFT achieves competitiveness with HEFA only under optimal conditions (maximum process capacity and high CO_2 prices) in the conservative scenario. In contrast, HTL demonstrates competitiveness at a lower process capacity of 2,500 t_{db}/d, with less dependence on feedstock availability and lower sensitivity to CO_2 price volatility. Under the progressive scenario, GFT reaches price silimar with Jet A1 (€0.50/L) only under optimal conditions. HTL, however, achieves a similar price at a capacity of 2,250 t_{db}/d, and at maximum capacity shows a 28% discount compared to its fossil counterpart.

Although these outcomes are promising, they must be interpreted with caution, as a certain degree of uncertainty remains. In particular, input parameters related to technological learning and progressive scenarios require further study to reduce this uncertainty. While studies suggest positive feedstock availability scenarios for 2050, additional work is needed to account for potential price increases driven by rising demand and the growing reliance on renewable feedstocks in the coming decades. Furthermore, economic feasibility is also influenced by price elasticity effects, including how increases in jet fuel prices may affect customer behavior and responses to price fluctuations. On the negative side, high electricity prices and higher labor wages are less ideal for full-scale SAF production in the Netherlands.

This study demonstrates the potential for commercial-scale SAF production in the Netherlands, but highlights that contributions from governments, fuel producers, and airlines at the global level are essential to make this feasible. A major opportunity lies in the untapped technological learning rate of GFT and HTL. To capitalize on this potential, governments should collaborate with fuel producers to accelerate deployment by providing subsidies that lower the capital burden of early-stage plants and reduce SAF prices to HEFA price levels. The analysis shows that HTL requires nearly seven times less subsidy support than GFT, with estimated needs of €1.16 B compared to €7.78 B. On the demand side, airlines should partner with fuel producers by securing offtake agreements for SAF produced

in new plants. Governments can further support this by investing in (airport) infrastructure needed for SAF refueling and rewarding airlines with higher SAF uptake through preferential access to airport slots.

With SAF blending mandates approaching in 2030 under the European Commission, it is only a matter of time before the aviation industry must fully commit to investing in new SAF production technologies. This study shows that the Netherlands is a feasible location for such developments. By 2050, HTL proved to be the most promising pathway for SAF production. However, the transition to a sustainable aviation sector will require collective action that extends beyond technological solutions alone.

Acronyms & Abbreviations

db = Dry basis
FT = Fischer-Tropsch
GFT = Gasification Fischer-Tropsch
HTL = Hydrothermal liquefaction
FP = Fast pyrolysis
CHP = Combined heat and power
BtL = Biomass-to-liquid
NOAK = nth-of-a-kind
FOAK = first-of-a-kind
MFSP = Minimum fuel selling price
SAF = Sustainable aviation fuel
APEA = Aspen Plus Economic Analyzer
WGS = Water–gas shift
LTFT = Low temperature Fischer-Tropsch
LT = Low temperature
HT = High temperature
WWT = Waste water treatment
sEF = Simple E-factor
cEF = Complete E-factor
DCFRR= Discounted cash flow rate of return
CapEx = Capital Expenditures
OpEx = Operating Expenditures
TCI = Total capital investment
TIC = Total installed cost
TPEC = Total purchase equipment cost
IC = Indirect costs
TDIC = Total direct and indirect Cost
LF = Location factor
WC = Working capital
DW&B = Direct wages and benefits
MW&B= Maintenance wages and benefits
MS&B = Maintenance salaries and benefits
NPV = Net present value
TLF = Technology learning factor
LPG = Liquefied petroleum gas
PSA = Pressure swing adsorption
Q = Capacity
h = Hour
d = Day
y = Year
GJ = Gigajoule
PJ = Petajoule
L = Liter

7 REFERENCES

[1] P. S. Jaramillo, *Climate Change 2022: Mitigation of Climate Change* (Cambridge University Press, Cambridge, New York) (2022), doi:10.1017/9781009157926.012, contribution of Working Group III to the Sixth Assessment Report of the IPCC.

[2] International Energy Agency, "Aviation," (2025), URL https://www.iea.org/energy-system/transport/aviation.

[3] IATA, "Disappointingly Slow Growth in SAF Production," https://www.iata.org/en/pressroom/2024-releases/2024-12-10-03/ (2024 dec), vol. 60, p. 1.

[4] R. de Vries, R. E. Wolleswinkel, M. Hoogreef, R. Vos, "A New Perspective on Battery-Electric Aviation, Part II: Conceptual Design of a 90-Seater," Tech. rep., AIAA SCITECH 2024 FORUM (2024), doi:0.2514/6.2024-1490.

[5] Airbus, "ZEROe: our hydrogen-powered aircraft," (2025), URL https://www.iea.org/energy-system/transport/aviation.

[6] ATAG, "Waypoint 2050: Aviation Industry's Climate Goals," (2021), URL https://aviationbenefits.org/media/167417/w2050_v2021_27sept_full.pdf.

[7] European Parliament and Council, "Regulation (EU) 2023/2405 on ensuring a level playing field for sustainable air transport (ReFuelEU Aviation)," https://eur-lex.europa.eu/legal-content/EN/TXT/?uri=CELEX%3A32023R2405 (2023), official Journal of the European Union.

[8] IATA, "Ramping up SAF through standalone HEFA facilities," Tech. rep., IATA (November 2024).

[9] S. van Dyk, J. Saddler, "Progress in Commercialization of Biojet / Sustainable Aviation Fuels (SAF)," Tech. rep., IEA Bioenergy (2024).

[10] A. Blanshard, M. McCurdy, S. Chokhani, "Fueling Net Zero. How the aviation industry can deploy sufficient sustainable aviation fuel to meet climate ambitions," Tech. rep., ATAG Waypoint 2050 (September 2021), URL https://aviationbenefits.org/media/167495/fueling-net-zero_september-2021.pdf.

[11] P. Ibarra-Gonzalez, B. G. Rong, "A review of the current state of biofuels production from lignocellulosic biomass using thermochemical conversion routes," *Chinese Journal of Chemical Engineering*, pp. 1523–1535 (2019).

[12] D. Carpenter, T. L. Westover, S. Czernik, W. Jablonski, "Biomass feedstocks for renewable fuel production: a review of the impacts of feedstock and pretreatment on the yield and product distribution of fast pyrolysis bio-oils and vapors," *Green Chemistry*, pp. 384–406 (2014).

[13] D. Cronin, A. J. Schmidt, J. Billing, T. R. Hart, S. P. Fox, X. Fonoll, J. Norton, M. R. Thorson, "Comparative Study on the Continuous Flow Hydrothermal Liquefaction of Various Wet-Waste Feedstock Types," *ACS*

Sustainable Chemistry Engineering (2022), doi:10.1021/acssuschemeng.1c07214.

[14] Y. Zhu, S. A. Tjokro Rahardjo, C. Valkenburg, L. J. Snowden-Swan, S. B. Jones, M. A. Machinal, "Techno-economic Analysis for the Thermochemical Conversion of Biomass to Liquid Fuels," Tech. rep., PNNL (2011).

[15] I. Tews, Y. Zhu, C. Drennan, D. Elliott, L. Snowden-Swan, K. Onarheim, D. Beckman, "Biomass Direct Liquefaction Options: TechnoEconomic and Life Cycle Assessment," Tech. rep., PNNL, Washington (2014).

[16] J. Lindblad, J. Routa, J. Ruotsalainen, M. Kolström, A. Isokangas, L. Sikanen, "Weather based moisture content modelling of harvesting residues in the stand," *Silva Fennica* (2018), doi:https://doi.org/10.14214/sf.7830.

[17] A. Krogh, "From Biomass to Sustainable Liquid Fuels: A Comparative Assessment of Conversion Pathways, Their Economic and Environmental Impacts, and Large-Scale Integration in the Future Energy System," (2024).

[18] W.-C. Wang, Y.-C. Liu, R. A. Nugroho, "Techno-economic analysis of renewable jet fuel production: The comparison between Fischer-Tropsch synthesis and pyrolysis," *Energy*, p. 121970 (2022).

[19] L. Verduzco, J. Ramírez, M. Amezcua-Allieri, "Techno-economic Analysis and Life Cycle Assessment of Sustainable Aviation Fuel (SAF) Production." *Sustainable Aviation Fuels. Sustainable Aviation* (2025), doi:https://doi.org/10.1007/978-3-031-83721-0_13.

[20] K. Tzanetis, J. Posada, A. Ramirez, "Analysis of biomass hydrothermal liquefaction and biocrude-oil upgrading for renewable jet fuel production: The impact of reaction conditions on production costs and GHG emissions performance," *Renewable Energy*, pp. 1388–1398 (2017).

[21] L. Snowden-Swan, R. Hallen, Y. Zhu, T. Hart, M. Bearden, J. Liu, T. Seiple, K. Albrecht, S. Jones, S. Fox, A. Schmidt, G. Maupin, J. Billing, D. Elliott, "Conceptual Biorefinery Design and Research Targeted for 2022: Hydrothermal Liquefaction Processing of Wet Waste to Fuels," Tech. rep., PNNL (2017).

[22] A. Kumar, J. D. Watkins, D. Cronin, A. J. Schmidt, D. M. Santosa, Z. Yang, J. Heyne, P. J. Valdez, "Hydrothermal liquefaction of wastewater-grown algae to produce synthetic aviation fuel: A combined experimental study and techno-economic assessment," *Energy Conversion and Management* (2025).

[23] R. d. S. Deuber, J. M. Bressanin, D. S. Fernandes, H. R. Guimarães, M. F. Chagas, A. Bonomi, L. V. Fregolente, M. D. B. Watanabe, "Production of Sustainable Aviation Fuels from Lignocellulosic Residues in Brazil through Hydrothermal Liquefaction: Techno-Economic and Environmental Assessments," *Energies* (2023).

[24] S. Michailos, A. Bridgwater, "A comparative techno-economic assessment of three bio-oil upgrading routes for aviation biofuel production," *Int J Energy Res.* (2019), doi:https://doi.org/10.1002/er.4745.

[25] A. H. Tanzil, K. Brandt, M. Wolcott, X. Zhang, M. Garcia-Perez, "Strategic assessment of sustainable aviation fuel production technologies: Yield improvement and cost reduction opportunities," *Biomass and Bioenergy* (2021), doi:https://doi.org/10.1016/j.biombioe.2020.105942.

[26] European Commission, "About the EU ETS," (2025), URL `https://climate.ec.europa.eu/eu-action/carbon-markets/eu-emissions-trading-system-eu-ets/about-eu-ets_en#documentation`.

[27] KLM Royal Dutch Airlines, "KLM Annual Report 2024," (2024), URL `https://www.klmannualreport.com/wp-content/uploads/2025/04/KLM-Annual-Report-2024.pdf`.

[28] M. Boosten, J. Oldenburger, J. Kremers, J. van Briel, N. Spliethof, D. Borgman, "Beschikbaarheid van Nederlandse verse houtige biomassa in 2030 en 2050," Tech. rep., Stichting Probos, Wageningen (2018).

[29] C. J. Meerstadt, B. Piersma, "Feedstocks for sustainable aviation," Tech. rep., Royal NLR (2021).

[30] Jet-A1-Fuel, "Jet A1 price Netherlands," (2025), URL `https://jet-a1-fuel.com/price/netherlands-the`.

[31] M. Weiss, M. Junginger, M. K. Patel, K. Blok, "A Review of Experience Curve Analyses for Energy Demand Technologies," *Technological Forecasting and Social Change*, vol. 77, no. 3, pp. 411–428 (2010), doi:10.1016/j.techfore.2009.10.009.

[32] A. de Klerk, "Fischer-Tropsch fuels refinery design," *Energy & Environmental Science*, p. 1177 (2011).

[33] S. Tanzer, J. Posada, S. Geraedts, A. Ramírez, "Lignocellulosic marine biofuel: Technoeconomic and environmental assessment for production in Brazil and Sweden," *Journal of Cleaner Production*, vol. 239, p. 117845 (2019).

[34] P. Spath, A. Aden, T. Eggeman, M. Ringer, B. Wallace, J. Jechura, ""Biomass to Hydrogen Production Detailed Design and Economics Utilizing the Battelle Columbus Laboratory Indirectly-Heated Gasifier," (2005), doi:10.2172/15016221.

[35] R. Bain, "Material and Energy Balances for Methanol from Biomass Using Biomass Gasifiers," Tech. rep. (1992).

[36] H. Hiller, R. Reimert, et al., "Gas Production," *Ullmann's Encyclopedia of Industrial Chemistry* (2006), doi:10.1002/14356007.a12_169.pub2.

[37] P. Häussinger, R. Lohmüller, A. Watson, "Hydrogen," *Ullmann's Encyclopedia of Industrial Chemistry* (2000), doi:10.1002/14356007.a13_297.

[38] E. C. Tan, M. Talmadge, A. Dutta, J. Hensley, J. Schaidle, M. Biddy, D. Humbird, L. J. Snowden-Swan, J. Ross, D. Sexton, *et al.*, "Process Design and Economics for the Conversion of Lignocellulosic Biomass to Hydrocarbons via Indirect Liquefaction. Thermochemical Research Pathway to High-Octane Gasoline Blendstock Through Methanol/Dimethyl Ether Intermediates," Tech. rep., NREL (National Renewable Energy Laboratory (NREL) (2015), doi:10.2172/1215006, URL `https://www.osti.gov/biblio/1215006`.

[39] S. Anutoiu, I. Dosa, D. C. Petrilean, "Steam turbine efficiency assessment, first step towards sustainable

electricity production," *MATEC Web Conf.* (2021), doi: https://doi.org/10.1051/matecconf/202134204007.

[40] T. M. Sakuneka, A. de Klerk, R. J. J. Nel, A. D. Pienaar, "Synthetic jet fuel production by combined propene oligomerization and aromatic alkylation over solid phosphoric acid," *Ind. Eng. Chem. Res.* (2008).

[41] T. M. Sakuneka, A. de Klerk, R. J. J. Nel, "Benzene reduction by alkylation in a solid phosphoric acid catalyzed olefin oligomerization process," *Ind. Eng. Chem. Res.* (2008).

[42] Y. Zhu, M. J. Biddy, S. B. Jones, D. C. Elliott, A. J. Schmidt, "Techno-economic analysis of liquid fuel production from woody biomass via hydrothermal liquefaction (HTL) and upgrading," *Applied Energy* (2014), doi: https://doi.org/10.1016/j.apenergy.2014.03.053.

[43] J. Wang, J. Wang, X. Liu, M. Chong, D. Cheng, F. Chen, "Oxidative Dehydrogenation of Cyclohexane Over Halogen-Decorated Ceria Nanorods with Tuned Electronic Structure and Surface Oxygen Species," *ChemCatChem* (2025), doi:https://doi.org/10.1002/cctc.202402059.

[44] A. A. Greish, A. P. Barkova, E. D. Finashina, T. Salmi, L. M. Kustov, "Selective dimerization of cyclohexene over a Re2O7-B2O3/Al2O3 catalyst under mild conditions," *Molecular Catalysis* (2021), doi:10.1016/j.mcat.2021.111398.

[45] A. Owusu-Boakye, "TWO-STAGE AROMATICS HYDROGENATION OF BITUMEN-DERIVED LIGHT GAS OIL," *University of Saskatchewan* (2005).

[46] T. Kasza, P. Solymosi, Z. Varga, I. Horáth, J. Hancsók, "Investigation of Isoparaffin Rich Alternative Fuel Production," *Chemical Engineering Transactions* (2011).

[47] D. J. C. Constable, A. D. Curzons, V. L. Cunninghama, "Metrics to 'green' chemistry—which are the best?" *Green Chemistry* (2002), doi:https://doi.org/10.1039/B206169B.

[48] D. Sangaré, M. Moscosa-Santillan, A. Aragón Piña, "Hydrothermal carbonization of biomass: experimental study, energy balance, process simulation, design, and techno-economic analysis," *Biomass Conv. Bioref.* (2024), doi:https://doi.org/10.1007/s13399-022-02484-3.

[49] R. Sheldon, M. Bode, S. Akakios, "Metrics of green chemistry: Waste minimization," *Current Opinion in Green and Sustainable Chemistry* (2022), doi:https://doi.org/10.1016/j.cogsc.2021.100569.

[50] M. van der Spek, A. Ramirez, A. Faaij, "Challenges and Uncertainties of Ex Ante Techno-Economic Analysis of Low TRL CO_2 Capture Technology: Lessons from a Case Study of an NGCC with Exhaust Gas Recycle and Electric Swing Adsorption," *Applied Energy*, vol. 208, pp. 920–934 (2017), doi:10.1016/j.apenergy.2017.09.058.

[51] C. Greig, A. Garnett, J. Oesch, S. Smart, "Guidelines for Scoping and Estimating Early Mover CCS Projects," *Univ. Queensl.* (2014).

[52] S. Andrea, B. Dina, "Development and Deployment of advanced biofuel demonstration facilities," Tech. rep., IEA Bioenergy: Task 39 (December 2024).

[53] E. W. Merrow, "An Analysis of Cost Improvement in Chemical Process Technologies," Tech. rep., Santa Monica, CA (1989), URL https://www.rand.org/content/dam/rand/pubs/reports/2006/R3357.pdf.

[54] W. Hettinga, H. Junginger, S. Dekker, M. Hoogwijk, A. McAloon, K. Hicks, "Understanding the reductions in US corn ethanol production costs: an experience curve approach," *Energy Policy* (2009), doi:https://doi.org/10.1016/J.ENPOL.2008.08.002.

[55] O. Cavalett, M. Chagas, T. Junqueira, M. Watanabe, A. Bonomi, "Environmental impacts of technology learning curve for cellulosic ethanol in Brazil." *Ind. Crop. Prod.* (2017), doi:https://doi.org/10.1016/J.INDCROP.2016.11.025.

[56] J. Van den Wall Bake, M. Junginger, A. Faaij, T. Poot, A. Walter, "Explaining the experience curve: cost reductions of Brazilian ethanol from sugarcane." *Biomass Bioenergy* (2009), doi:https://doi.org/10.1016/J.BIOMBIOE.2008.10.006.

[57] R. Weber, L. Snowden-Swan, "The economics of numbering up a chemical process enterprise," *J Adv Manuf Process* (2019), doi:https://doi.org/10.1002/amp2.10011.

[58] W. D. Seider, D. R. Lewin, J. D. Seader, S. Widagdo, *Product and Process Design Principles: Synthesis, Analysis and Evaluation* (Wiley), 3rd ed. (2010).

[59] R. M. Swanson, J. A. Satrio, R. C. Brown, A. Platon, D. D. Hsu, "Techno-Economic Analysis of Biofuels Production Based on Gasification," Tech. rep., National Renewable Energy Laboratory, Colorado (2010).

[60] Intratec, "Netherlands Plants Location Factor," (2020), URL https://www.intratec.us/solutions/industry-economics-worldwide/plant-location-factor/netherlands-plant-location-

[61] Norton Rose Fulbright, "The 2025 Dutch tax plan: Impact on businesses," (2024 September).

[62] X.-S. Yang, *Engineering Mathematics with Examples and Applications* (Academic Press) (2017).

[63] National Energy Technology Laboratory (NETL), "Technology Learning Curve (FOAK to NOAK): Quality Guidelines for Energy System Studies," Tech. rep., U.S. Department of Energy (2013).

[64] Centraal Plan Bureau (CPB), "Choosing for the future: Four scenarios for 2050," Tech. rep. (2024).

[65] Ipsos IO, "Onderzoek 'Week van het Vakmanschap'," Tech. rep. (2025).

[66] Stillwater Associates, "Sky-High Cost of Compliance: EU's SAF Mandate Prices Unveiled," (2025), URL https://stillwaterassociates.com/sky-high-cost-of-compliance-eus-saf-mandate-pric?cn-reloaded=1.

[67] Nederlandse Emissieautoriteit (NEA), "Algemeen Energie voor Vervoer 2022-2030," (2025), URL https://www.emissieautoriteit.nl/onderwerpen/hernieuwbare-energie-voor-vervoer/algemeen-hernieuwbare-energie-voor-vervoer.

[68] M. van der Spek, A. Ramirez, A. Faaij, ", improving uncertainty evaluation of process models by using pedigree analysis. A case study on CO2 capture with

monoethanolamine," *Computers Chemical Engineering* (2016), doi:https://doi.org/10.1016/j.compchemeng.2015.10.006.

[69] F. Yang, Y. Yao, "Sustainable aviation fuel pathways: Emissions, costs and uncertainty," *Resources, Conservation and Recycling* (2025), doi:https://doi.org/10.1016/j.resconrec.2025.108124.

[70] National Research Council (US) Chemical Sciences Roundtable, "Impact of Advances in Computing and Communications Technologies on Chemical Science and Technology: Report of a Workshop," *National Academies Press (US)* (1999), doi: https://www.ncbi.nlm.nih.gov/books/NBK44989/.

Appendix A

Please see supplementary material for the Microsoft Excel® spreadsheet model.

Appendix B

Pedigree Matrix - Technical Model

Gasification Fischer-Tropsch

Pedigree / Criterion	Proxy		Emperical Basis		Theoretical Understanding		Methodological Rigor	
	Mean	Std. Dev.	Mean	Std. Dev.	Mean	Std. Dev.	Mean	Std. Dev.
Process Design	3.00	0.00	2.33	0.47	3.67	0.47	2.67	0.47
Process variables	2.50	0.41	2.50	0.41	3.00	0.00	2.67	0.47
Mass balance	2.83	0.24	2.17	0.24	3.33	0.47	2.67	0.47
Energy balance	2.50	0.41	2.17	0.24	3.00	0.00	2.33	0.47

Hydrothermal Liquefaction

Pedigree / Criterion	Proxy		Emperical Basis		Theoretical Understanding		Methodological Rigor	
	Mean	Std. Dev.	Mean	Std. Dev.	Mean	Std. Dev.	Mean	Std. Dev.
Process Design	3.00	0.00	2.00	0.00	3.67	0.47	2.67	0.47
Process variables	2.50	0.41	2.33	0.47	3.00	0.00	2.67	0.47
Mass balance	2.50	0.41	2.17	0.24	3.33	0.47	2.67	0.47
Energy balance	3.00	0.00	2.25	0.25	3.00	0.00	3.00	0.00

Pedigree Matrix - Economic Model

Gasification Fischer-Tropsch

Pedigree / Criterion	Proxy		Emperical Basis		Theoretical Understanding		Methodological Rigor	
	Mean	Std. Dev.	Mean	Std. Dev.	Mean	Std. Dev.	Mean	Std. Dev.
Financial Model	3.00	0.00	2.33	0.47	3.67	0.47	3.00	0.00
Fixed Operating Cost	3.33	0.47	2.33	0.94	3.67	0.47	2.67	0.47
Variable Operating Cost	2.50	0.41	2.50	0.41	3.67	0.47	2.83	0.62
Total Capital Investment	3.00	0.00	2.67	0.47	3.67	0.47	3.00	0.00
Technological Learning	2.50	0.50	2.00	1.00	3.50	0.50	2.50	0.50
Capital Expenditures	2.67	0.47	2.00	0.00	3.67	0.47	3.17	0.62

Hydrothermal Liquefaction

Pedigree / Criterion	Proxy		Emperical Basis		Theoretical Understanding		Methodological Rigor	
	Mean	Std. Dev.	Mean	Std. Dev.	Mean	Std. Dev.	Mean	Std. Dev.
Financial Model	3.00	0.00	2.33	0.47	3.67	0.47	3.00	0.00
Fixed Operating Cost	3.00	0.00	2.33	0.94	3.67	0.47	2.67	0.47
Variable Operating Cost	2.50	0.41	2.50	0.41	3.67	0.47	2.83	0.62
Total Capital Investment	3.00	0.00	2.67	0.47	3.67	0.47	3.00	0.00
Technological Learning	2.50	0.50	2.00	1.00	3.50	0.50	2.50	0.50
Capital Expenditures	2.33	0.47	2.00	0.00	3.67	0.47	3.17	0.62

Legend
3.5-4.0
3.0-3.49
2.5-2.99
2.0-2.49
1.5-1.99
1.0-1.49

Fig. 10. Resulting matrices of Pedigree Analysis.

2

Research Proposal

Nomenclature

Abbreviation	Definition
BtL	Biomass-to-Liquid
CEPCI	Chemical Engineering Plant Cost Index
FOAK	First-of-a-kind
FP	Fast pyrolysis
FT	Fischer-Tropsch
GHG	Greenhouse gas
HTL	Hydrothermal liquefaction
IRR	Internal rate of return
MFSP	Minimum fuel selling price
MSOW	Municipal solid organic waste
SAF	Sustainable aviation fuel
TCC	Thermochemical conversion
TEA	Techno-economic analysis

2.1. Introduction and Relevance of the Project

Direct greenhouse gas (GHG) emissions from transport sector accounted for 23% of total global emissions in 2019. 12% of transport emissions came from aviation. These emissions continue to grow rapidly with rates of around 2.5% per year [1], largely due to the sector's near-complete reliance, 99.7%, on fossil-based kerosene and overall growing demand for flying [2]. Decarbonizing the aviation sector has become a critical global challenge. Sustainable Aviation Fuels (SAF), derived from advanced renewable biofuels, are increasingly seen as a key solution to reducing aviation emissions [3].

The growing interest in SAF is driven by international policy targets that mandate progressive SAF blending alongside fossil kerosene. In particular, the European Union's ReFuelEU Aviation mandate requires that SAF usage at EU airports increase from 2% in 2025 to 70% by 2050 [4]. This creates a strong demand for scalable, economically viable SAF production technologies across Europe.

Currently, advanced biofuels can be produced from lignocellulosic biomass sources. Early generations of biofuels, derived from food crops, have been associated with several potential drawbacks, including net energy losses, increased GHG emissions, and rising food prices. This has shifted attention toward the development of second-generation biofuels produced from non-food lignocellulosic feedstocks such as forestry residue, municipal solid organic waste (MSOW), and wheat straw [5]. The availability and selection of biomass feedstock are highly dependent on geographical location, which plays a primary role in determining viable input streams for biofuel production [6].

These feedstocks are converted into biofuels through multiple thermochemical conversion technologies, collectively referred to as biomass-to-liquid (BtL) pathways. Prior to conversion, biomass undergoes pretreatment steps, such as drying and grinding, to improve process efficiency and handling. The pretreated biomass is then processed through key thermochemical conversion technologies, including gasification followed by Fischer–Tropsch (FT) synthesis, fast pyrolysis (FP), and hydrothermal liquefaction (HTL). However, the oil products generated by these processes (syngas or bio-oil) do not yet meet the specifications of drop-in SAF. Therefore, additional upgrading processes are required, followed by product separation into fractions suitable for jet fuel, diesel, and gasoline applications.

In this context, the Netherlands, with its strategic position and the presence of a major international hub at Amsterdam Airport Schiphol, represents an attractive location for SAF production and distribution. The increasing demand driven by EU mandates, combined with anticipated feedstock availability in the Netherlands [7], highlights the need for a focused techno-economic evaluation of suitable BtL pathways under Dutch conditions.

2.2. Literature Review

A thorough literature study is performed to understand thermochemical technologies, evaluate system & process designs, techno-economic analysis methodologies, process data sources, feedstock availability, and jet fuel refining designs. A review of current knowledge and research gaps are given in order to specify a relevant research that contributes to the knowledge domain.

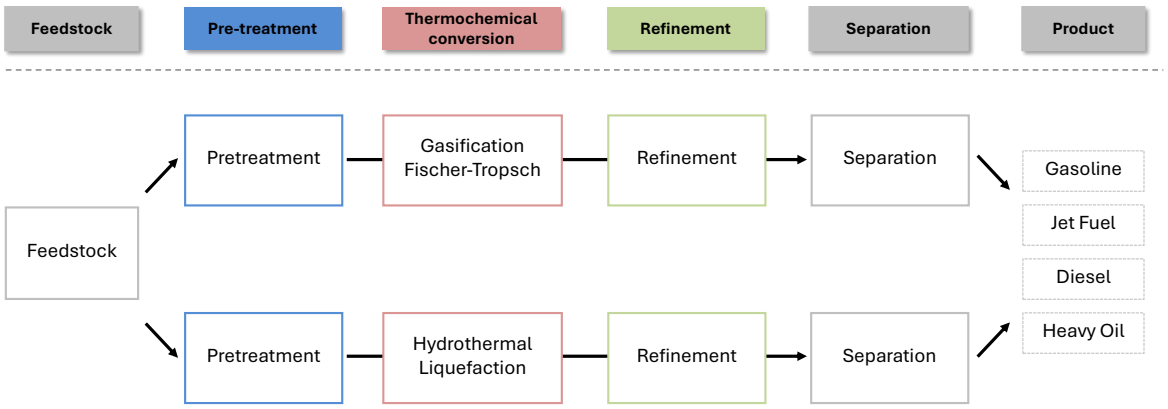

Figure 2.1: System overview showing two pathways including their thermochemical conversion technologies; gasification Fischer-Tropsch and hydrothermal liquefaction. The product streams (gasoline, jet fuel, diesel, and heavy oil) are shown aggregated for visual clarity; in practice, these outputs are not aggregated.

Thermochemical conversion technology (TCC) process design can be divided into three stages: pretreatment, thermochemical conversion, and refinery. In this study, three thermochemical conversion technologies are assessed: gasification Fischer-Tropsch (FT), fast pyrolysis (FP), and hydrothermal liquefaction (HTL). Biomass pretreatment is necessary to optimize its composition, improve process efficiency, and enhance fuel yield. Pretreatment operations includes drying and size reduction [8], where HTL only needs size reduction, as drying is unnecessary due to the process's aqueous operating environment [6].

To enhance the performance of aviation biofuel production, various biomass pretreatment methods, such as cell rupture, can be applied to improve the availability of biomass components and increase reaction yields. Ash and protein removal are often considered to reduce undesirable compounds in the resulting bio-oil and aviation biofuel, particularly ash and nitrogenous compounds, which can negatively impact fuel quality. However, these advanced pretreatment methods are not included in this research due to the limited availability of consistent data in the literature. Moreover, excluding these processes ensures a fair and comparable evaluation of different thermochemical conversion technologies (TCCs) [9]. Only grinding and drying steps are incorporated.

The pretreated feedstock is then directed to the thermochemical conversion stage, where lignocellulosic biomass is transformed into intermediate products: syngas for gasification, and bio-oil for FP and HTL. Gasification FT involves converting biomass into syngas (a mixture of CO and H_2) through partial oxidation at high temperatures (600–1000°C), followed by catalytic FT synthesis to produce syncrude suited as feedstock for renewable fuels. Fast pyrolysis rapidly heats biomass in the absence of oxygen (450–600°C) to generate bio-oil, non-condensable gases, and char, with bio-oil being the primary product for further refinement. HTL, on the other hand, processes biomass in hot, pressurized water (300–400°C, 5–20 MPa), breaking down complex biomass structures into a bio-oil product that requires further refining [10].

Once converted into syncrude or bio-oil, further refinement is required to make it suitable for transportation fuels. Processes such as hydrotreating remove oxygen and impurities, hydrocracking breaks down heavy molecules into lighter fuel fractions, and distillation separates the final products into gasoline, diesel, and jet fuel. Refining design is based on precursor technology, syncrude/bio-oil composition, target product [6]. Further details will be discussed in the literature section about refinery.

2.2.1. Biomass-to-Liquid Techno-Economic Analysis Studies

Several studies have assessed the system illustrated in Figure 1. Some focus on the techno-economic analysis of a single pathway, others compare multiple feedstocks, while some provide only technical designs and evaluations. In summary, a substantial body of literature exists that addresses either individual components or the entire system, each using its own methodology. A common thread in techno-economic evaluation papers is that the biomass-to-liquid (BtL) system is modelled using mass and energy balances derived from software simulations or experimental data from research laboratories and pilot plants. These mass and energy balances define the interconnections between unit operations by accounting for all material and energy inputs and outputs, forming the foundation of any BtL system description. The data generated from these balances can then be manipulated to represent a certain scenario, incorporating variables such as, target fuel product, process scale, and economic assumptions. This scenario can be evaluated through a techno-economic analysis, in which capital and operational costs are estimated using data derived from the mass and energy balances. Based on these costs the minimum fuel selling price (MFSP) can be determined, providing a basis for assessing the economic viability of the system. Finally, a sensitivity analysis can be performed to determine which parameters have the greatest impact on the MFSP.

Liu et al. [11] conducted a system & process design evaluation for a FP plant in Taiwan, aimed at converting rice husk into renewable jet fuel. Rice husk was considered as feedstock as this is the most abundant agricultural waste in Taiwan. The reference year for economic assumptions was set to 2017, with all prices adjusted accordingly. The process scale was set at a feedstock input of 600 tonnes per day which can be seen as a 'first-of-a-kind' (FOAK) facility, whereas commercial-scale (nth-of-a-kind) plants typically range between 1,000-2,000 tonnes per day. Process data was obtained using the Aspen Plus simulation tool and applied to estimate equipment sizes for the projected plant. Capital costs were sourced from quotations provided by real-world equipment vendors, while operational costs were derived from mass and energy balance outputs. MFSP was calculated based on the condition of a net present value (NPV) of zero, with an integrated internal rate of return, a commonly applied method for evaluating plant financial feasibility [12]. The renewable jet fuel produced in this study demonstrated an energy yield[1] of 26.8%, a mass yield of 9.2%, and an MFSP of $3.21 per liter, which remains approximately 6 to 9 times higher than U.S. fossil jet fuel prices in 2017 [13]. Furthermore, a sensitivity analysis revealed that feedstock (rice husk) costs had the greatest impact on MFSP variability, with 43% of the operating costs attributed to feedstock acquisition.

Wang et al. [14] expanded on the previously mentioned study by conducting a system & process design evaluation for the gasification FT pathway. The methodology, system, and scenario parameters were intentionally kept consistent to enable a direct comparison between both conversion routes. The gasification FT process yielded renewable jet fuel with an energy efficiency of 42.5%, a mass yield of 14.4%, and an MFSP of $2.20 per liter. In techno-economic terms, this pathway outperformed fast pyrolysis, evaluated in the previous study. Similar to the earlier findings, feedstock costs exhibited the highest sensitivity on the MFSP, with 49% of the total operating costs attributed to feedstock acquisition.

Tanzer et al. [15] conducted a screening study that generated first-order estimates of the techno-economic performance of 33 scenarios for producing biofuels for marine applications. The study considered three thermochemical conversion technologies: gasification FT, FP, and HTL. It considers nine different locally sourced biomass feedstocks for two plant locations: Sweden and Brazil. Biofuel production was modelled for a 500 tonnes per day FOAK plant, with the base year set to 2020. In addition to the structure outlined in Figure 1, each technology pathway included the coproduction of heat, electricity, and hydrogen. The study further assumes that undistilled syncrude bio-oil is directly blendable into marine fuels. Rather than designing and simulating its own computational process models, the study relied on process data sourced from literature, pilot plants, and laboratory-scale testing specific to each feedstock-technology combination. Where data was unavailable, parameter values were extrapolated based on informed estimates. A parallel data structure was used to ensure that each feedstock-technology pathway employed a standardized set of assumptions and parameters. Data and calculations were aggregated into an interlinked spreadsheet model, enabling comparison across a large set of scenarios. Capital and operating costs were estimated using literature and mass balance data, and the MFSP was calculated based on plant break-even conditions, accounting for capital de-

[1] Yield is calculated for feedstock-to-jet fuel conversion

preciation but excluding internal rate of return. The results indicated that the estimated MFSP ranged between 2.5 and 8 times the current price of marine fuel. Across all scenarios, capital depreciation, maintenance, and feedstock acquisition represented the largest contributions to operating costs. Sensitivity analysis confirmed these factors as the main drivers of volatility in the MFSP.

Tzanetis et al. [16] conducted a system & process design evaluation for biomass-to-biofuel conversion using HTL and FP. The study examined seven different process conditions: six for HTL, varying in catalyst composition and reaction temperature, and one for FP. The analysis was based on a 1,000 tonnes per day plant located in Sweden, utilizing forest residues as feedstock due to its local availability. The economic evaluation was conducted with 2014 as the reference year. Process data was obtained from a computer simulation model designed in Aspen Plus. For both HTL and pyrolysis pathways, the same bio-oil upgrading process was applied, with an assumed product distribution of 24% gasoline, 40% jet fuel, 14% diesel, and 22% heavy oil. Capital and operating costs were estimated based on equipment purchase costs as a function of equipment sizing and were supported by mass and energy balances. Although the study focused on sustainable aviation fuel (SAF) production, no specific MFSP values were reported. Instead, total production costs for the full product mix were provided, with the most cost-effective process condition resulting in a production cost of €0.80/L ($1.04/L). Internal rate of return was not factored into these calculations. Sensitivity analysis showed that feedstock costs and capital investment were the dominant contributors to production cost variability.

The degree of energy efficiency and resource circularity varies among BtL systems, with more advanced configurations integrating these practices to improve sustainability and economic performance. Recent studies have made significant efforts to optimize circular resource use, though their approaches differ. For example, **Tanzer et al.** [15] presents a state-of-the-art system that incorporates a cogeneration plant, utilizing excess solid residues from the thermochemical conversion (TCC) processes to produce electricity. Additionally, the system includes internal hydrogen production from process gases, which is used for the hydrotreatment of FP and HTL-derived bio-oils. The system boundaries also account for wastewater treatment, flue gas handling, and ash disposal, all included in the operational cost structure. **Tzanetis et al.** [16] also designed a circular system where solid residues from fast pyrolysis and HTL are combusted to use heat internally to feed the TCC, also internal hydrogen production is included from waste gases from TCC process. Flue gases are used as internal heat however the disposal of the gases is unclear. Wastewater treatment costs are included. **Liu et al.** [11] and **Wang et al.** [14] does not use gaseous and solid residues for internal use but sells them as by-products to lower the operating costs. Excess CO2 was vented into the atmosphere, which is not circular.

2.2.2. Process Data Sources

Mass and energy balances can be seen as the foundation of any BtL system. Studies that did not develop their own detailed process models, or only did so partially, often rely on these foundational models, which are mostly designed by large research institutions specialized on renewable fuels technologies . The key advantage of these models is that they provide comprehensive, well-documented process designs that can serve as reliable data sources for techno-economic evaluations.

Several foundational studies are widely referenced in this context. **Zhu et al.** [8] evaluated five fuel production pathways, including gasification FT, fast pyrolysis, and HTL, using a consistent process design to compare different biomass conversion technologies. **Wright et al.** [17] focused on biomass conversion through fast pyrolysis, both with and without integrated hydrogen production. **Swanson et al.** [18] investigated biomass conversion using both low- and high-temperature gasification FT systems, including electricity as a co-product. Finally, **Tews et al.** [19] presented detailed process designs for both fast pyrolysis and HTL-based biomass conversion pathways.

2.2.3. Biomass Feedstock Availability

Most BtL studies in the literature commonly select forestry residues (woody materials) as the primary feedstock [15, 19, 16]. This preference is driven by a combination of factors: high availability, relatively low cost, low ash content, and the ability to produce high-quality bio-oil, making forestry residues particularly well-suited for thermochemical conversion processes [20]. Currently, forestry residues are less abundant in the Netherlands [21]. However, **Boosten et al.** [7] evaluated the future availability of woody biomass under different scenarios for 2030 and 2050. For the Netherlands in 2050, the study

projected an annual availability of 1324 kilotonnes (dry basis) of woody biomass for bioenergy purposes. The report further identified oak and beech as the most common species in the country. In line with this, the European Union has declared that woody biomass is an eligible feedstock for the production of advanced biofuels, including renewable jet fuels [4]. The Dutch Emissions Authority is responsible for enforcing these regulations in the Netherlands and also has published information outlining the eligible feedstocks applicable to advanced biofuel production [22].

2.2.4. Refinery Design

The design of the upgrading process is critical in converting bio-oil into sustainable aviation fuel (SAF) that meet industry specifications. Jet-A fuel, used in commercial aviation, must adhere to strict quality standards [23]. Unprocessed bio-oil, however, lacks the required properties, including low energy density and high moisture content, making it unsuitable for direct use as jet fuel [6].

In gasification FT pathways, upgrading involves multiple unit operations such as hydrocracking and hydroisomerization, as demonstrated by **Wang et al.** [14]. For fast pyrolysis and HTL-derived bio-oils, upgrading typically involves hydrotreatment processes, including hydrogenation, hydrogenolysis, and hydrodeoxygenation, to achieve the desired fuel properties [11, 16]. Despite targeting jet fuel production, these processes still yield significant fractions of gasoline, diesel, and heavy oils.

Klerk [24] presents an advanced refinery design focused on maximizing jet fuel output from gasification FT products. This design integrates unit operations such as oligomerization, alkylation, hydrotreatment, aromatization, and hydrocracking. These steps serve to increase aromatic content to meet jet fuel specifications, adjust the carbon chain length to the kerosene boiling range, and introduce branching in molecular structures to lower freezing points, all essential characteristics for jet fuel. The result is a mass yield of 62.7% from FT products to jet fuel, a substantial improvement compared to the 41.9% yield reported by **Wang et al.** [14] for gasification FT-based jet fuel production.

After hydrotreatment of pyrolysis and HTL bio-oils, the resulting product mixture typically consists of gasoline, diesel, and heavy oil, with only a portion of these fractions meeting jet fuel specifications. This jet fuel fraction can potentially be maximized through additional upgrading processes; however, no studies to date have explored jet fuel maximization strategies for fast pyrolysis and HTL-derived products. Nonetheless, existing refinery technologies offer pathways for this optimization. Lighter fractions, such as gasoline-range hydrocarbons, can be upgraded through oligomerization [25] and alkylation [26] to increase carbon chain length into the kerosene boiling range. Similarly, hydrocracking can be applied to heavier fractions, such as diesel and heavy oils, to break down long-chain hydrocarbons into smaller molecules suitable for jet fuel [27].

Recent research increasingly focuses on integrating HTL biocrude into existing refineries through co-processing [28, 29]. Studies show that hydrotreatment can effectively stabilize HTL biocrude, enabling blending with current refinery streams for the production of jet and diesel range hydrocarbons. However, this study does not investigate co-processing. Instead, it focuses on stand-alone BtL pathways, primarily because more detailed and validated process data is available for these systems.

2.2.5. Research Gaps & Scope

The literature describes various biomass-to-liquid (BtL) systems and their individual components. However, two key research gaps can be identified: a scenario-based one, and technical-based one.

As outlined in the introduction, the demand for sustainable aviation fuel (SAF) is rapidly increasing in the Netherlands, while current feedstock options for SAF production remain limited. This highlights the need to explore alternative feedstocks for renewable fuel production. According to projections by **Boosten et al.** [7], the availability of forestry residues (woody biomass) in the Netherlands is expected to increase significantly over the coming decades, reaching approximately 1,324 kilotonnes per year by 2050. This feedstock is particularly well-suited for thermochemical conversion processes due to its favourable properties, including low ash content and high bio-oil yield potential [20]. Theoretically, utilizing this biomass could cover up to 4.4% of the Netherlands' total SAF demand in 2050, based on biomass-to-SAF yield data reported in the literature [21, 14]. However, fuel yield alone is not sufficient to determine the viability of these pathways. To date, no comprehensive techno-economic analysis has been conducted comparing gasification FT, FP, and HTL processes for SAF production under Dutch

conditions. Therefore, an in-depth techno-economic analysis is required, comparing these process designs within the context of a 2050 scenario in the Netherlands, using forestry residues as the primary feedstock. The analysis will assume a commercial-scale (nth-of-a-kind) plant with a processing capacity of 2,000 tonnes per day.

The second research gap concerns the maximization of SAF production through the design of a dedicated, tailor-made refinery. As highlighted in the literature review, **Klerk** [24] presents a refinery configuration specifically designed to maximize SAF yield from gasification FT products. However, while this approach could also be adapted for the upgrading of bio-oils derived from fast pyrolysis and HTL, no studies to date have explored this application. Developing such refinery designs for these pathways could enhance SAF production potential in the Netherlands. This leads to the following research objective.

The research objective is to assess the economic feasibility of Sustainable Aviation Fuel (SAF) production process in the Netherlands in 2050, aimed to optimize SAF yield, in the Netherlands by performing a comparative techno-economic analysis of gasification Fischer-Tropsch and hydrothermal liquefaction plant design, using forestry residues as feedstock.

2.2.6. Research Question

Under which conditions is the production of SAF from forestry residues economically feasible in the Netherlands by 2050, when aiming to maximize SAF yield through gasification FT and HTL at commercial scale?

- **Subquestion 1:** How can refinery designs for each pathway be tailored to maximize SAF output, and what unit operations are required for this optimization?
- **Subquestion 2:** How do the three thermochemical pathways compare in terms of mass and energy yields, and MFSP for SAF production in the Netherlands by 2050?
- **Subquestion 3:** Which parameters (e.g., feedstock costs, plant scale, utility costs) have the largest impact on the economic viability and MFSP for each pathway?

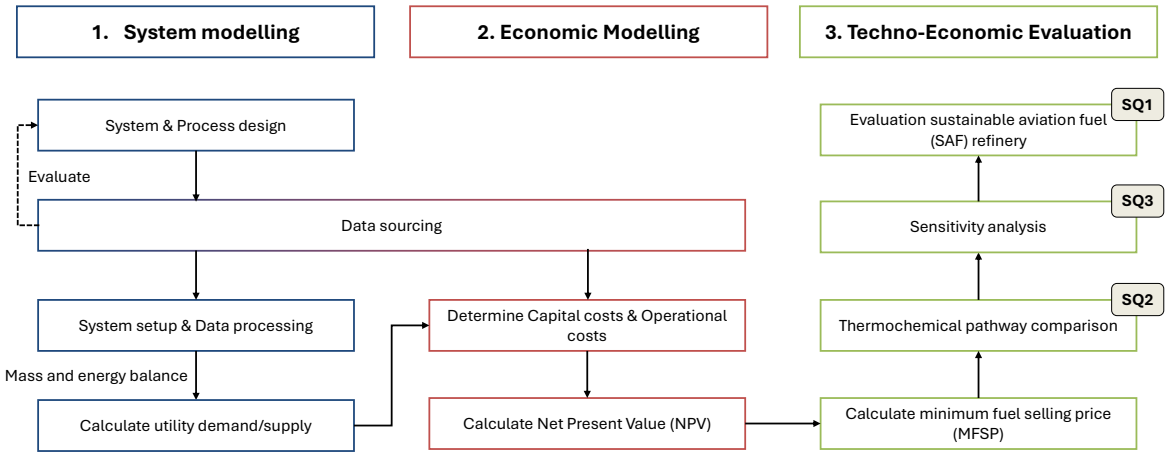

Figure 2.2: An overview of the methodology divided into three phases: System modelling, Economic modelling, and Techno-economic evaluation. Where applicable, certain blocks are linked to specific research sub-questions (SQ) that are addressed during this phase or step.

2.3. Methodology

This section outlines the methodology applied in this research, as illustrated in Figure 2. The methodology is developed by combining elements from various studies, integrating relevant approaches to address the main research question and its sub-questions. In addition, the methodology directly supports achieving the research objective. It is structured into three main phases: System modelling, Economic modelling, and Techno-economic evaluation.

System modelling follows the methodology described by **Tanzer et al.** [15], in which the biomass-to-liquid (BtL) system is represented as a unit-process black box model with a consistent level of detail across all unit operations. Thermochemical process designs and mass and energy balances are sourced from existing literature, with careful selection based on similarity in process conditions, data quality, and relevance to the chosen technology-feedstock combinations — gasification Fischer-Tropsch (FT), fast pyrolysis (FP), and hydrothermal liquefaction (HTL) using woody biomass. The objective of this approach is not to replicate detailed process simulations in specialized software, but to focus on the key parameters that influence jet fuel yield and total production costs.

2.3.1. System Modelling

The first step in system modelling is system design, where key assumptions regarding system boundaries are defined. These include the plant capacity, set at 2,000 tonnes per day, as well as parameters such as residue stream handling, target fuel products, feedstock type, country of reference, and base year. The economic base year is set to 2025, while feedstock availability is assumed at projected 2050 levels for the Netherlands. This choice avoids the uncertainty associated with long-term price forecasting, as extrapolations to 2050 would require excessive assumptions, reducing the reliability of the economic evaluation.

Process design involves defining the unit operations for each thermochemical pathway. Foundational models from the literature, including those by **Zhu et al.**, **Wright et al.**, **Swanson et al.**, **Tews et al.** [8, 17, 18, 19] form the core of this design approach. These models are widely referenced in the field and provide well-documented, high-quality process data, making them suitable for adaptation in this research. However, these models do not include a dedicated sustainable aviation fuel (SAF) refinery design. Therefore, data and configurations for the SAF tailored refinery are sourced from additional literature, including **Klerk**, **Gorimbo et al.**, **Sakuneka et al.**, **Zhang et al.** [24, 25, 26, 27].

Once the system and process design is completed, the data sourcing phase collects all required data, including mass and energy balances, for the proposed system. As outlined in the previous section, much of this data is provided by the foundational models. Any data gaps will be addressed through additional literature sources or complementary datasets. All data sources will be carefully referenced to

ensure transparency and enhance the reproducibility of the research. A feedback loop is incorporated into the methodology, allowing for the system and process design to be re-evaluated and adjusted if certain data proves unavailable or inconsistent. The system setup phase involves the quantitative description of the BtL system. This is implemented in Microsoft Excel, which is widely used in similar research due to its ability to generate consistent and comparable results across a large set of scenarios through the use of an interlinked spreadsheet model. Excel is particularly convenient because it allows for transparent calculations, easy adjustment of assumptions, and clear visualization of mass and energy balances. Additionally, this software aligns with the researcher's expertise, ensuring efficient and accurate model development. Source data is entered and processed within the spreadsheet, and where specific data is unavailable, values are carefully extrapolated based on relevant literature and justified assumptions.

This system setup results mass and energy balances for the final system and process design, incorporating all assumptions that define the system boundaries. These balances also produce a detailed utility demand and supply profile, outlining the consumption of key resources such as electricity, hydrogen, natural gas, cooling water, steam, and catalysts. In some cases, the system may also generate surplus utilities — for example, excess electricity produced by a co-generation plant utilizing process residue streams — which are accounted for as part of the utility supply.

2.3.2. Economic Modelling

The second phase is economic modelling, which follows the methodology outlined by **Liu et al.** and **Wang et al.** [11, 14]. In this study, it is assumed that the Net Present Value (NPV) is zero, meaning the plant operates at the break-even point. The NPV calculation incorporates capital investments, net cash flows, and the internal rate of return (IRR), providing a comprehensive measure of the economic feasibility of the BtL system. In the study **Tanzer et al.** [15], the internal rate of return (IRR) was not included in the economic assessment, resulting in an incomplete representation of the overall economic feasibility.

First, the capital and operational costs are determined. Within operational costs, a distinction is made between variable and fixed costs. Variable operating costs are derived from the utility demand and supply profiles established in phase 1 (System modelling) and are assigned price values based on sourced data. Fixed operating costs include expenses such as salaries, labour burden, maintenance, and other overheads, with prices determined using financial assumptions supported by data from literature and data sourcing efforts.

Capital costs are primarily based on values provided in foundational studies. When capital cost data is available, it is adjusted to the appropriate economic base year using the Chemical Engineering Plant Cost Index (CEPCI) [30]. The CEPCI approach is consistent with the methods used by **Tanzer et al.** and **Tzanetis et al.** [15, 16]. It differs, however, from the methodology applied by **Liu et al.** and **Wang et al.** [11, 14], where capital costs were directly obtained from real-world vendor quotations. When capital costs cannot be found in foundational studies, it is sourced from additional literature, with this effort undertaken during the data sourcing phase.

2.3.3. Techno-Economic Evaluation

Phase 3 consists of the techno-economic evaluation, where the minimum fuel selling price (MFSP) is calculated following the methodology outlined in Phase 2. A comparative assessment of the different thermochemical pathways — gasification FT, fast pyrolysis, and HTL — is conducted, evaluating energy yields, mass yields, and associated costs. Subsequently, a sensitivity analysis is performed, varying key parameters such as utility costs, capital costs, and plant capacity. This approach follows the methodology applied in the studies referenced in Phase 2. The sensitivity analysis allows for the identification of parameters with the greatest influence on the MFSP. The results of the techno-economic evaluation will be presented and supported by quantitative data, primarily in the form of graphs, to clearly illustrate and compare the performance of the three pathways.

Finally, an evaluation of the sustainable aviation fuel (SAF) refinery design is carried out to determine its economic benefits. This is achieved by comparing the tailored refinery design to a baseline scenario where the refined fractions (gasoline, diesel, and heavy oil) are sold as separate products without further upgrading toward jet fuel.

2.3.4. Data Management

Below a overview of expected data and results are given in a table.

Type of data	**File format(s)**	**How will data be collected (for re-used data: source and terms of use)?**	**Purpose of processing**	**Storage location**	**Who will have access to the data**
BtL-system model	.csv file, .xlsx file	Data will be collected by a literature review. Sources will be referenced in the specific cells and will also be aggregated in a separate worksheet.	To create a BtL-system model to perform techno-economic analysis	Project storage location (OneDrive)	Mark ter Heide, supervisors, chair
Aspen Plus models	apw.	Data will be collected by literature review. Sources will be referenced.	To create mass- and energy balance data and utility profile data	Project storage location (Onedrive)	Mark ter Heide, supervisors

Table 2.2: Data management plan

2.4. Planning

See the Gantt chart in the Appendix. The project is structured into four distinct phases:

1. **Literature Review & Research Definition (Weeks 1–6)**
   During this phase, a comprehensive literature review is conducted, extracting essential knowledge in the following areas:
   - Thermochemical process knowledge
   - System & process designs
   - Techno-economic analysis methodologies
   - Process data sources
   - Feedstock availability
   - Tailored jet fuel refining designs

   Milestone: Research Proposal Review Meeting (Week 6)
2. **Research Phase 1 (Weeks 7–16)**
   In this phase, system and process design are carried out, including the formulation of key system assumptions that define the system boundaries. Process design activities are performed, and relevant data is sourced to quantitatively describe the system in Microsoft Excel. All findings and the applied methodology are thoroughly documented to ensure transparency and reproducibility of results.
   Milestone: Mid-Term Meeting (Week 15)
3. **Research Phase 2 (Weeks 17–27)**
   This phase focuses on refining system setup and data processing, calculating utility demand and supply, and sourcing additional data. Capital and operational costs are determined, and financial evaluations such as net present value (NPV) and minimum fuel selling price (MFSP) are performed. A thermochemical pathway comparison and sensitivity analysis are conducted, alongside an evaluation of sustainable aviation fuel (SAF) refinery integration. The phase concludes with continuous documentation and submission of the draft thesis.
   Milestones: Finalization System Model (Week 18), Submission of Draft Thesis (Week 27)
4. **Research Dissemination (Weeks 28–33)**
   All research findings are compiled and documented in preparation for the Green Light Review. Following this, efforts focus on finalizing the thesis and preparing for the defence.
   Milestones: Green Light Review (Week 29), Thesis Defence (Week 33)

2.5. Conclusion

The increasing urgency to decarbonize the aviation sector highlights the need for scalable and economically viable sustainable aviation fuel (SAF) production technologies. This research proposal has outlined a comprehensive approach to evaluate the techno-economic feasibility of producing SAF in the Netherlands by 2050 using gasification Fischer–Tropsch (FT), fast pyrolysis (FP), and hydrothermal liquefaction (HTL) pathways. The focus on forestry residues as a feedstock aligns with projected availability and regulatory frameworks. A comparative analysis is performed for these pathways and this addresses two key research gaps; a Dutch scenario in 2050 for SAF production from biomass, and SAF tailored refinery design to maximize this fraction.

The choice to focus on forestry residues as the primary biomass feedstock is based on projections of future availability within the Dutch context, in alignment with EU and national regulatory frameworks that promote the use of lignocellulosic biomass for advanced biofuel production. This research addresses two key gaps identified in current literature. First, there is a lack of scenario-based analysis for SAF production under Dutch conditions in the year 2050, considering projected biomass availability. Second, the potential of refinery configurations specifically designed to maximize the SAF fraction from each conversion route remains underexplored. System and process modelling are carried out using established methodologies and process designs sourced from validated literature, complemented by mass and energy balances. These balances are critical to quantify utility demands such as electricity, steam, hydrogen, and cooling water. Economic evaluation is performed through the calculation of the minimum fuel selling price (MFSP), using a net present value (NPV) method that incorporates capital expenditure, operational costs, and financial assumptions over the plant's lifetime.

A comprehensive sensitivity analysis is conducted to identify and quantify the influence of key parameters, including feedstock cost, plant scale, utility prices, and capital costs, on the MFSP. In addition, an assessment of SAF tailored refinery configurations is performed.

Bibliography

[1] Jaramillo, P. S., *Climate Change 2022: Mitigation of Climate Change*, Cambridge University Press, Cambridge, New York, 2022, Contribution of Working Group III to the Sixth Assessment Report of the IPCC.

[2] IATA, "Disappointingly Slow Growth in SAF Production," https://www.iata.org/en/pressroom/2024-releases/2024-12-10-03/, dec 2024, Vol. 60, p. 1.

[3] Wang, B., Ting, Z. J., and Zhao, M., "Sustainable aviation fuels: Key opportunities and challenges in lowering carbon emissions for aviation industry," *Carbon Capture Science & Technology*, 2024, pp. 100263.

[4] European Parliament and Council, "Regulation (EU) 2023/2405 on ensuring a level playing field for sustainable air transport (ReFuelEU Aviation)," https://eur-lex.europa.eu/legal-content/EN/TXT/?uri=CELEX%3A32023R2405, 2023, Official Journal of the European Union.

[5] Cronin, D., Schmidt, A. J., Billing, J., Hart, T. R., Fox, S. P., Fonoll, X., Norton, J., and Thorson, M. R., "Comparative Study on the Continuous Flow Hydrothermal Liquefaction of Various Wet-Waste Feedstock Types," *ACS Sustainable Chemistry Engineering*, 2022.

[6] Ibarra-Gonzalez, P. and Rong, B. G., "A review of the current state of biofuels production from lignocellulosic biomass using thermochemical conversion routes," *Chinese Journal of Chemical Engineering*, 2019, pp. 1523–1535.

[7] Boosten, M., Oldenburger, J., Kremers, J., van Briel, J., Spliethof, N., and Borgman, D., "Beschikbaarheid van Nederlandse verse houtige biomassa in 2030 en 2050," Tech. rep., Stichting Probos, Wageningen, 2018.

[8] Zhu, Y., Tjokro Rahardjo, S. A., Valkenburg, C., Snowden-Swan, L. J., Jones, S. B., and Machinal, M. A., "Techno-economic Analysis for the Thermochemical Conversion of Biomass to Liquid Fuels," Tech. rep., PNNL, 2011.

[9] Marangon, B. B., Castro, J. S., and Calijuri, M. L., "Aviation fuel based on wastewater-grown microalgae: Challenges and opportunities of hydrothermal liquefaction and hydrotreatment," *Journal of Environmental Management*, 2024, pp. 120418.

[10] Krogh, A. E. M., "Method for comparing efficiency and system integration potential for biomass-based fuels production pathways," *Journal of Cleaner Production*, 2022, pp. 134336.

[11] Liu, Y.-C. and Wang, W.-C., "Process design and evaluations for producing pyrolytic jet fuel," *Biofuels, Bioproducts and Biorefining*, 2020, pp. 249–264.

[12] Capaz, R. S., Guida, E., Seabra, J. E., Osseweijer, P., and Posada, J. A., "Mitigating carbon emissions through sustainable aviation fuels: costs and potential," *Biofuels, Bioproducts and Biorefining*, 2020, pp. 502–524.

[13] U.S. Energy Information Administration, "U.S. Kerosene Wholesale/Resale Price by Refiners," https://www.eia.gov/dnav/pet/hist/LeafHandler.ashx?n=PET&s=EMA_EPPK_PWG_NUS_DPG&f=M, March 2025.

[14] Wang, W.-C., Liu, Y.-C., and Nugroho, R. A., "Techno-economic analysis of renewable jet fuel production: The comparison between Fischer-Tropsch synthesis and pyrolysis," *Energy*, 2022, pp. 121970.

[15] Tanzer, S., Posada, J., Geraedts, S., and Ramírez, A., "Lignocellulosic marine biofuel: Technoeconomic and environmental assessment for production in Brazil and Sweden," *Journal of Cleaner Production*, Vol. 239, 2019, pp. 117845.

[16] Tzanetis, K., Posada, J., and Ramirez, A., “Analysis of biomass hydrothermal liquefaction and biocrude-oil upgrading for renewable jet fuel production: The impact of reaction conditions on production costs and GHG emissions performance,” *Renewable Energy*, 2017, pp. 1388–1398.

[17] Wright, M. M., Satrio, J. A., Brown, R. C., Daugaard, D. E., and Hsu, D. D., “Techno-Economic Analysis of Biomass Fast Pyrolysis to Transportation Fuels,” Tech. rep., National Renewable Energy Laboratory, Colorado, 2010.

[18] Swanson, R. M., Satrio, J. A., Brown, R. C., Platon, A., and Hsu, D. D., “Techno-Economic Analysis of Biofuels Production Based on Gasification,” Tech. rep., National Renewable Energy Laboratory, Colorado, 2010.

[19] Tews, I., Zhu, Y., Drennan, C., Elliott, D., Snowden-Swan, L., Onarheim, K., and Beckman, D., “Biomass Direct Liquefaction Options: TechnoEconomic and Life Cycle Assessment,” Tech. rep., PNNL, Washington, 2014.

[20] Carpenter, D., Westover, T. L., Czernik, S., and Jablonski, W., “Biomass feedstocks for renewable fuel production: a review of the impacts of feedstock and pretreatment on the yield and product distribution of fast pyrolysis bio-oils and vapors,” *Green Chemistry*, 2014, pp. 384–406.

[21] Meerstadt, C. J. and Piersma, B., “Feedstocks for sustainable aviation,” Tech. rep., Royal NLR, 2021.

[22] Nederlandse Emissieautoriteit, “Referentiegegevens REV,” `https://www.emissieautoriteit.nl/onderwerpen/register/referentiegegevens#anker-2-grondstoffen-in-het-rev`, March 2025.

[23] Air BP, “Handbook of Products,” `https://web.archive.org/web/20110608075828/http://www.bp.com/liveassets/bp_internet/aviation/air_bp/STAGING/local_assets/downloads_pdfs/a/air_bp_products_handbook_04004_1.pdf`, 2000, Hemel Hempstead.

[24] de Klerk, A., “Fischer-Tropsch fuels refinery design,” *Energy & Environmental Science*, 2011, pp. 1177.

[25] Gorimbo, J., Moyo, M., and Liu, X., “Oligomerization of bio-olefins for bio-jet fuel,” *Hydrocarbon Biorefinery*, edited by S. K. Maity, K. Gayen, and T. K. Bhowmick, Elsevier, 2022, pp. 271–294.

[26] Sakuneka, T. M., de Klerk, A., Nel, R. J. J., and Pienaar, A. D., “Synthetic jet fuel production by combined propene oligomerization and aromatic alkylation over solid phosphoric acid,” *Ind. Eng. Chem. Res.*, 2008.

[27] Zhang, X., Chen, Q., Zhang, Q., Wang, C., Ma, L., and Xu, Y., “Conversion of pyrolytic lignin to aromatic hydrocarbons by hydrocracking over pristine MoO3 catalyst,” *Journal of Analytical and Applied Pyrolysis*, 2018, pp. 60–66.

[28] Dimitriadis, A. and Bezergianni, S., “Towards Bio-Crude Refinery Integration: Hydrodeoxygenation and Co-Hydroprocessing with Light Cycle Oil,” *Energies*, 2024, pp. 6032.

[29] Lindfors, C., Elliott, D., Prins, W., Oasmaa, A., and Lehtonen, J., “Co-processing of Biocrudes in Oil Refineries,” *Energy & Fuels*, 2019, pp. 799–804.

[30] Chemical Engineering, “Chemical engineering plant cost Index,” `https://www.chemengonline.com/pci-home`, 2025.

A

Gantt Chart

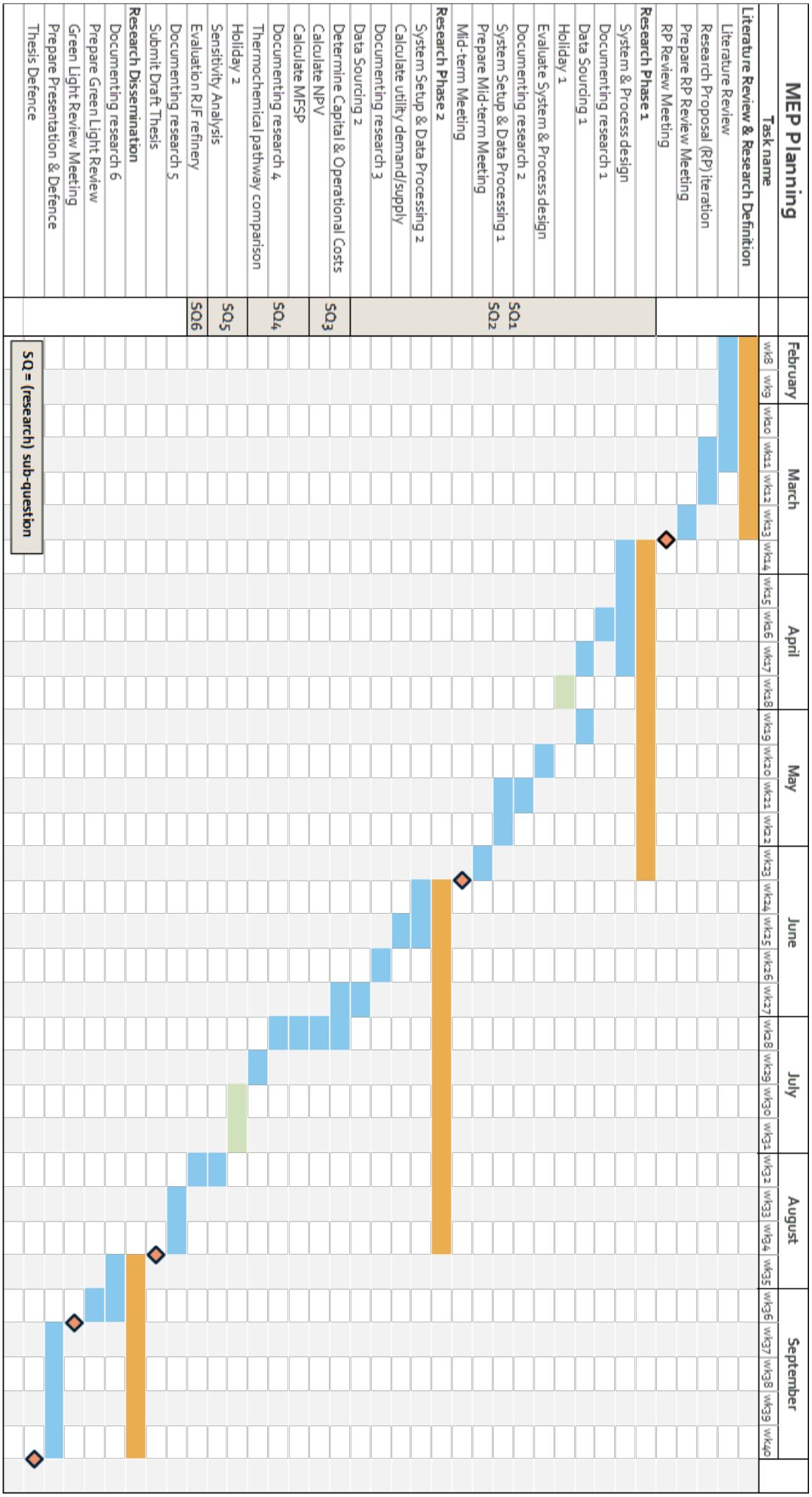
MEP Planning
Task name
February
March
April
May
June
July
August
September
wk8 wk9 wk10 wk11 wk12 wk13 wk14 wk15 wk16 wk17 wk18 wk19 wk20 wk21 wk22 wk23 wk24 wk25 wk26 wk27 wk28 wk29 wk30 wk31 wk32 wk33 wk34 wk35 wk36 wk37 wk38 wk39 wk40
Literature Review & Research Definition
Literature Review
Research Proposal (RP) iteration
Prepare RP Review Meeting
RP Review Meeting
Research Phase 1
System & Process design
Documenting research 1
Data Sourcing 1
Holiday 1
Evaluate System & Process design
Documenting research 2
System Setup & Data Processing 1
Prepare Mid-term Meeting
Mid-term Meeting
Research Phase 2
System Setup & Data Processing 2
Calculate utility demand/supply
Documenting research 3
Data Sourcing 2
Determine Capital & Operational Costs
Calculate NPV
Calculate MFSP
Documenting research 4
Thermochemical pathway comparison
Holiday 2
Sensitivity Analysis
Evaluation RJF refinery
Documenting research 5
Submit Draft Thesis
Research Dissemination
Documenting research 6
Prepare Green Light Review
Green Light Review Meeting
Prepare Presentation & Defence
Thesis Defence
SQ1
SQ2
SQ3
SQ4
SQ5
SQ6
SQ = (research) sub-question